

Article

Design and Test of Disturbed Fertilizer Strip-Ejection Device with Vertical Pendulum Bar Based on Discrete Element Method

Lintao Chen ¹, Xiangwu Deng ^{2,*}, Zhaoxiang Liu ¹, Xiangwei Mou ¹, Xu Ma ³ and Rui Chen ¹¹ Department of Mechanical Engineering, Guangxi Normal University, Guilin 541004, China² College of Electronic Information Engineering, Guangdong University of Petrochemical Technology, Maoming 525000, China³ College of Engineering, South China Agricultural University, 483 Wushan Road, Guangzhou 510642, China

* Correspondence: dengxiangwu2019@gdupt.edu.cn

Abstract: Fertilizer can improve the yield of crops per unit area, and uniform fertilizer discharge can improve the fertilizer utilization rate. Therefore, it is meaningful to improve the performance of fertilizer-discharge devices in order to improve the modernization level of crop field fertilizer management. To address the problems of operational smoothness, stability and poor uniformity of fertilizer discharge, and other difficult problems encountered with strip fertilizer-discharge devices, this study designs a disturbed fertilizer strip-discharge device with a vertical pendulum. The main factors affecting the performance of fertilizer discharge were the wedge angle of the push-disturbing main pendulum bar (PMPB), the inclination angle of the aided-stirring pendulum pick (APP), the flow gap of the pendulum bar (FGPB), and the operation frequency of the swing-rod combination (SRC). The discrete element method (DEM) was used to establish a simulation model of the fertilizer device to explore the influence of the main factors on the performance of fertilizer discharge, with the coefficient of variation (CV) of fertilizer discharge uniformity and fertilizer discharge accuracy (FDA) used as the evaluation indices. The results show that the factors affecting the CV of fertilizer discharge uniformity and FDA were, in order of priority, the operation frequency of the SRC, the FGPB, the wedge angle of the PMPB, and the inclination angle of the APP. The optimal parameters after rounding were as follows: the wedge angle of the PMPB was 45°, the inclination angle of the APP was 46°, the operation frequency of the SRC was 188 times/min, and the FGPB was 4.5 mm. At this point, the model predicted that the CV of fertilizer discharge uniformity would be 10.53%, and that the FDA would be 3.19%. Using the optimal parameters for bench test verification, it was found that the wedge angle of the PMPB was 45°, the inclination angle of the APP was 46°, the operation frequency of the SRC was 188 times/min, the FGPB was 4.5 mm, the CV of the uniformity of the fertilizer discharge was 11.06%, and the FDA was 3.51%. In the test, the fertilizer-discharge device was stable and had good adaptability to different fertilizers. The results of this study can provide a theoretical reference for the development of precision strip-fertilizer application devices.

Keywords: granular fertilizers; strip-fertilizer application; fertilizer discharge; perturbation; vertical pendulum bar



Citation: Chen, L.; Deng, X.; Liu, Z.; Mou, X.; Ma, X.; Chen, R. Design and Test of Disturbed Fertilizer Strip-Ejection Device with Vertical Pendulum Bar Based on Discrete Element Method. *Agriculture* **2024**, *14*, 635. <https://doi.org/10.3390/agriculture14040635>

Academic Editor: John M. Fielke

Received: 7 March 2024

Revised: 14 April 2024

Accepted: 18 April 2024

Published: 20 April 2024



Copyright: © 2024 by the authors. Licensee MDPI, Basel, Switzerland. This article is an open access article distributed under the terms and conditions of the Creative Commons Attribution (CC BY) license (<https://creativecommons.org/licenses/by/4.0/>).

1. Introduction

Fertilizer can effectively increase crop yield, and fertilization is one of the important factors affecting crop yield. Reasonable fertilization is beneficial for crop growth and achieves the goals of stable yield and increased income [1]. The fertilizer utilization rate in China is only about 33%, and this can be effectively improved by improving the uniformity of fertilizer devices [2]. Therefore, such an improvement is significant for the modernization of crop field-fertilization management [1,2]. Granular fertilizers are widely used in crops around the world because of their good physical properties, ease of application, and long-lasting effects [2,3].

According to the type of fertilizer application in the field, fertilizer discharge devices can be divided into three types: broadcast-fertilization, hole-fertilization, and strip-fertilization devices [4]. The main equipment for broadcast fertilization includes centrifugal spreaders. Centrifugal spreaders generally use the centrifugal force generated by the rotation of a horizontal disc to sprinkle fertilizer, and they have the characteristics of a wide spraying range and high operational efficiency. A horizontal disc-type fertilizer-spraying device is used for spraying with a large working width [5]. These devices have been previously studied and are widely used in countries such as Europe and America [6]. Patterson [7] conducted a study on the movement of fertilizer on a fertilizer tray. Cool [8] constructed a motion model of fertilizer after leaving the disk and studied the influence of fertilizer rotation on its motion trajectory and landing point position in the air. Lv [9] designed a conical-disk fertilizer-spreading device, which requires the cooperation of large tractors and is suitable for plain areas. However, in broadcast-type devices, the lateral stability of fertilizer spraying is relatively low, and they are generally used for large-scale field base fertilizer and topdressing operations.

Hole fertilization devices can achieve fixed-point and quantitative fertilization in the root zone of crops [10]. An inclined trapezoidal hole-type quantitative fertilizer discharger has been designed [11]. Domestic scholars have also conducted research on hole-forming mechanisms for liquid fertilizer-hole application, large hole-type granular fertilizer hole-forming mechanisms, and intermittent motion slot-wheel hole-type fertilization mechanisms [12]. Hole fertilization consists of applying fertilizer at a predetermined position on one side of the crop or between two crops, so it is necessary to check the relative position of the seeds or crop seedlings with the fertilizer discharge port to ensure that the hole fertilization and fertilizer discharge position are within the predetermined range. Hole-application-type devices discharge fertilizer intermittently through special mechanisms, and the movement process is complex. At present, liquid fertilizer is mainly used for hole fertilization because it has good fluidity, strong stability, and uniform discharge.

Due to the fact that the current main grain or vegetable crops are mechanically sown or transplanted, crops are mainly distributed in linear rows [13]. Strip fertilization is suitable for different crops around the world. Strip-type fertilization devices are a type of side-deep fertilization technology, and they can apply fertilizer to soil layers at a certain depth, resulting in higher fertilizer utilization efficiency and easier precision fertilization operations [14]. In recent years, scholars have conducted extensive research on the structural form of fertilizer strippers to improve the uniformity of fertilizer application. In order to improve the precision and stability of strip fertilization devices, a PID controller was used [15]. To effectively improve the quality of strip fertilization, a fertilizer particle dynamic change model based on the discrete element method (EDM) was established to study the main factors affecting the uniformity and stability of fertilization [16]. However, the existing problems, such as the smoothness, stability, and poor uniformity of fertilizer discharge in the operation of strip fertilizer devices, are still not well solved. It is necessary to break through traditional methods and adopt new design ideas to improve operation performance. In response to the problems of poor smoothness, stability, and uniformity of fertilizer discharge in the operation of strip-fertilization devices, this study proposes a disturbed fertilizer strip-ejection device (DFSD) with a vertical pendulum bar. The fertilizer discharge device is optimized using a combination of mathematical modeling, discrete element simulation, and experimentation. The simulation model of the fertilizer strip device is established using EDEM. The influence of the main factors on the performance of fertilizer discharge is explored, and a trial production bench test is developed for experimental verification.

2. Materials and Methods

2.1. Overall DFSD Structure and Working Principle

2.1.1. Overall DFSD Structure

The proposed DFSD with a vertical pendulum bar mainly consists of a fertilizer discharge box, an eccentric pin shaft, a cover shell, an SRC, a fertilizer discharge port, a

closed door, and a shaft pad, as shown in Figure 1a. The swing rod combination (SRC) is located directly below the cover, and it includes a push-disturbing main pendulum bar (PMPB), aided-stirring pendulum picks (APPs) I and II, and a guide needle. APPs I and II are installed on both sides of the PMPB, with a certain degree of opening. The device is equipped with an eccentric pin shaft on the walking wheel of the fertilizer applicator to form a crank rocker transmission mechanism, which drives the SRC to perform a reciprocating motion, forcing fertilizer to flow out from the fertilizer discharge port [17,18]. The end of the PMPB is designed as a wedge, and it is a key component for pushing and moving fertilizer. The ends of APPs I and II are designed as conical surfaces, which can push the fertilizers on both sides towards the fertilizer-discharge port for continuous discharge. The upper end of the guide needle is hinged to the PMPB, and the lower end is inserted into the fertilizer-discharge port. As the PMPB moves, the guide needle moves up and down at the fertilizer-discharge port, preventing fertilizer arching. A displacement adjustment component is located at the fertilizer discharge port to change the amount of fertilizer discharged.

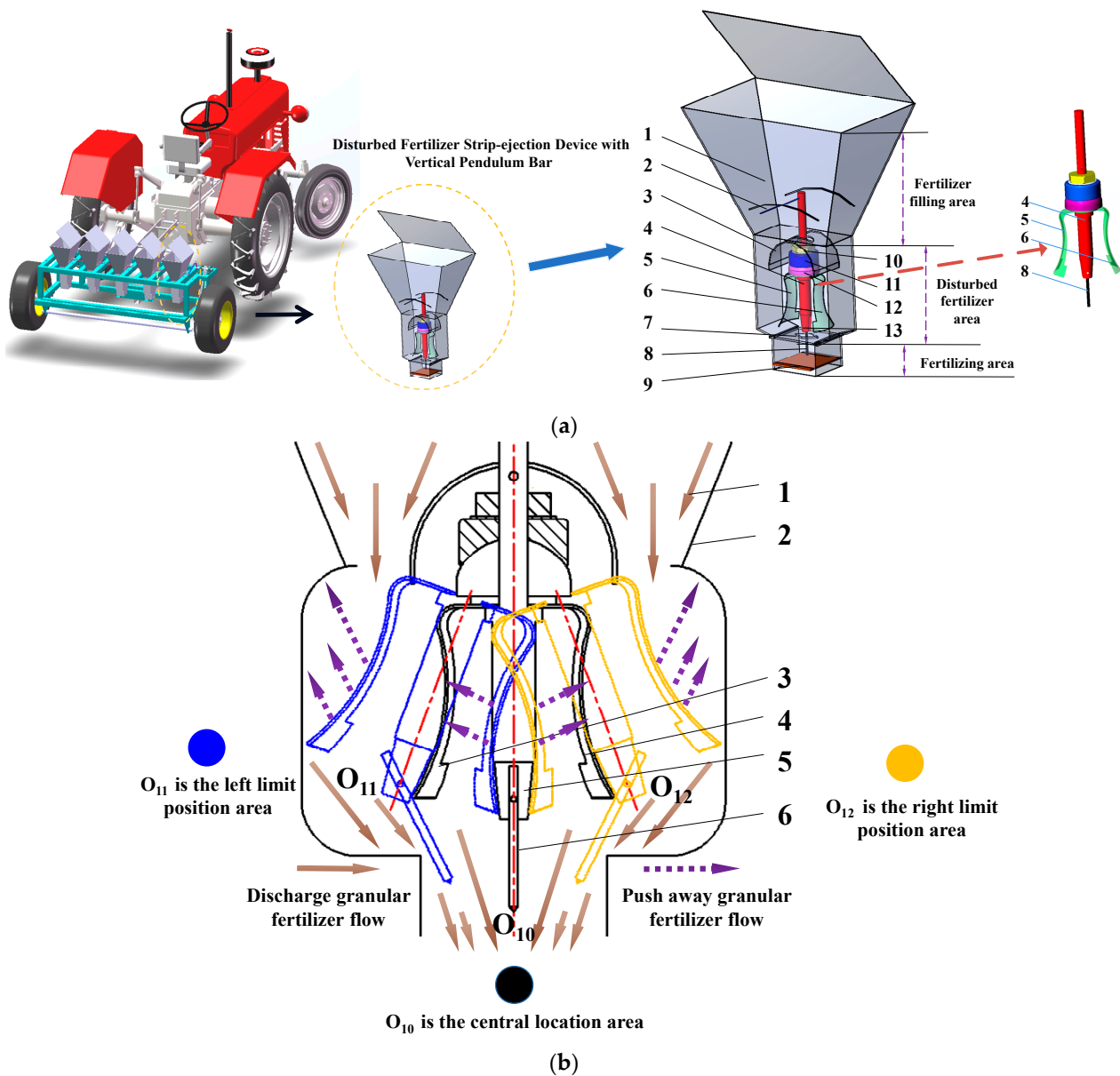


Figure 1. The structure and working process of disturbed fertilizer strip-ejection device with vertical pendulum bar: (a) The structure of DFSD: 1 Fertilizer-discharge box; 2 Eccentric pin; 3 Housing;

4 Push-disturbance main pendulum bar; 5 Aided-stirring pendulum pick I; 6 Aided-stirring pendulum pick II; 7 Fertilizer-discharge port; 8 Guide pin; 9 Closed door; 10 Fastening bolt; 11 Shaft pad; 12 Washer; 13 Articulation bit; (b) The working process of DFSD: 1 Fertilizer flow; 2 Fertilizer-discharge box; 3 Aided-stirring pendulum pick I; 4 Aided-stirring pendulum pick II; 5 The main pendulum bar; 6 Guide needle.

2.1.2. Working Principle

According to the working principle of fertilizer-discharge devices, the operating area of the device is divided into a fertilizer-filling area, a fertilizer-disturbing area, and a fertilizer-dropping area. An eccentric pin shaft is installed on the walking wheel of the fertilizer applicator to form a crank rocker-transmission mechanism, which drives the SRC to perform a reciprocating motion, forcing the fertilizer to flow out from the fertilizer discharge port. When the SRC is stationary, the fertilizer flows under gravity, and the amount of fertilizer discharged is controlled by the opening of the fertilizer outlet. When the SRC moves, the PMPB moves from the middle position O_{10} to the left or right extreme position zone O_{11} or O_{12} , and it continuously swings (as shown in Figure 1b). On the one hand, under the action of the PMPB and the ends of APPs I and II in the SRC, the fertilizer is pushed out of the fertilizer discharge port to form a continuous fertilizer flow. On the other hand, the fertilizer is pushed away from the fertilizer-discharge port to form a material-free zone. Under the action of gravity, it is filled with the surrounding fertilizer, causing the fertilizer to self-flow and discharge. The two complement each other, forming a precise fertilizer-discharge process.

2.2. Design and Analysis of Key Components

In order to improve the operational performance of the DFSD with a vertical pendulum bar, a parameter design and a theoretical analysis were conducted on key components, and the influence of the device's structural parameters on the movement of fertilizer particles were thoroughly studied. The theoretical analysis mainly included an analysis of SRC motion and a mechanical analysis.

2.2.1. Analysis of SRC Motion

The force situation of the fertilizer-discharge device during operation is complex. By conducting kinematic and dynamic analyses of its fertilizer-discharge process, studying the force situation of each part can aid in identifying the weak links of the system in executing the fertilizer-discharge action, determining the key factors affecting the fertilizer-discharge effect and providing a theoretical basis for optimizing structural parameters.

1. Motion Analysis of PMPB

The fertilizer-discharge performance depends on the motion characteristics of the SRC. According to the working principle and analysis of the fertilizer discharge device, the PMPB motion mechanism depends on the crank rocker mechanism motion, as shown in Figure 2a. According to the requirements of fertilization operation, the swing center of the PMPB is the center of the fertilizer discharge port. This is where the PMPB performs an isochronous motion, which means that the motion time in both reciprocating directions is equal [19]. The distance ratio of its reciprocating motion is 1:1, and it has a reciprocating stroke ratio coefficient of 1. The two dead points (A_1 and A_2) of Motion Point A are connected through the rotation center [20,21], and there are constraints between the four bars of the main swing rod motion mechanism:

$$L_1^2 = L^2 + r^2 - r_0^2 \quad (1)$$

where r refers to the crank radius, m; r_0 is the length of rocker arm, m; L_1 is the length of connecting rod, m; and L is the distance between the crank rotation center and the swing center, m.

The PMPB continuously swings under the action of the crank rocker mechanism, and its motion parameters are represented by angular displacement β and angular velocity ω .

For the convenience of analysis, taking the center of the crank motion as the origin and establishing a coordinate system, the motion equation of point A satisfies.

$$\begin{cases} x_A = r_0 \cos \beta_1 + L \cos \gamma \\ y_A = r_0 \sin \beta_1 - L \sin \gamma \end{cases} \quad (2)$$

$\beta_1 = \beta + \zeta$, where β is the angular displacement of the main swing bar (swing angle) ($^\circ$); β_1 is the angle between the main pendulum and the horizontal plane at motion point A ($^\circ$); and ζ is the angle between the main pendulum and the horizontal at dead center A_2 ($^\circ$).

According to the cosine theorem, the relationship of ΔOO_1A is solved:

$$L_2^2 = r_0^2 + L^2 + 2r_0L \cos(\beta_1 + \gamma) \quad (3)$$

Similarly, from the relationship solution of ΔAOB , the following formula can be obtained:

$$L_1^2 = r^2 + L_2^2 - 2rL_2 \cos(\alpha - \alpha_1) = r^2 + L_2^2 - 2rL_2(\cos \alpha \cos \alpha_1 + \sin \alpha \sin \alpha_1) \quad (4)$$

By substituting the formula $\cos \alpha_1 = x_A/L_2$, $\sin \alpha_1 = y_A/L_2$ into Equation (4) and combining Equations (1) to (3), the following Equation (5) is obtained:

$$r \cos(\beta_1 - \alpha) - L \cos(\beta_1 + \gamma) = r_0 - \frac{rL}{r_0} \cos(\alpha + \gamma) \quad (5)$$

By combining Equation (2) and substituting it into Equation (5), the angular displacement β is obtained

$$\beta = \arcsin \frac{r_0 - \frac{rL}{r_0} \cos(\alpha + \gamma)}{\sqrt{r^2 + L^2 - 2rL \cos(\alpha + \gamma)}} + \arctan \frac{L \cos \gamma - r \cos \alpha}{L \sin \gamma + r \sin \alpha} - \zeta \quad (6)$$

The explicit equation of Equation (5) is reorganized and shifted to form an equation that always equals 0, which is an implicit function. The purpose of doing this is to create a universal and standardized expression for subsequent mathematical analysis and processing. Furthermore, Equation (5) is written as implicit function $F(\beta_1, \alpha)$ of Equation (7) as follows:

$$F(\beta_1, \alpha) = r \cos(\beta_1 - \alpha) - L \cos(\beta_1 + \gamma) - r_0 + \frac{rL}{r_0} \cos(\alpha + \gamma) = 0 \quad (7)$$

By using the implicit function differentiation method, the angular velocity ω can be obtained.

$$\omega = \frac{d\beta}{dt} = \frac{r \sin(\beta_1 - \alpha) - \frac{rL}{r_0} \sin(\alpha + \gamma)}{r \sin(\beta_1 - \alpha) - L \sin(\beta_1 + \gamma)} \omega_0 \quad (8)$$

By using Equations (6)–(8), it can be determined that angular displacement β and angular velocity ω of the PMPB are related to the radius of the crank, r ; the length of the rocker arm, r_0 ; the distance L between the crank rotation center and the swing center; and the crank rotation angle, α . When the structural parameters of the fertilizer-discharge device (r , r_0 , and L) are constant, angular displacement β and angular velocity ω are only related to crank rotation angle α . When the structural parameters of the fertilizer-discharge device (radius of the crank, r ; length of the rocker arm, r_0 ; and distance, L , between the crank rotation center and the swing center) are constant, γ and ζ are constant. Thus, angular velocity ω of the PMPB is only related to crank rotation angle α . As the rotational speed of the crank rocker mechanism increases, angular velocity ω of the PMPB significantly increases. Displacement K and velocity S of the K-point at the end of the PMPB are calculated:

$$\begin{cases} S = \beta r_1 \frac{\pi}{180} \\ V = \frac{dS}{dt} = r_1 \omega \end{cases} \quad (9)$$

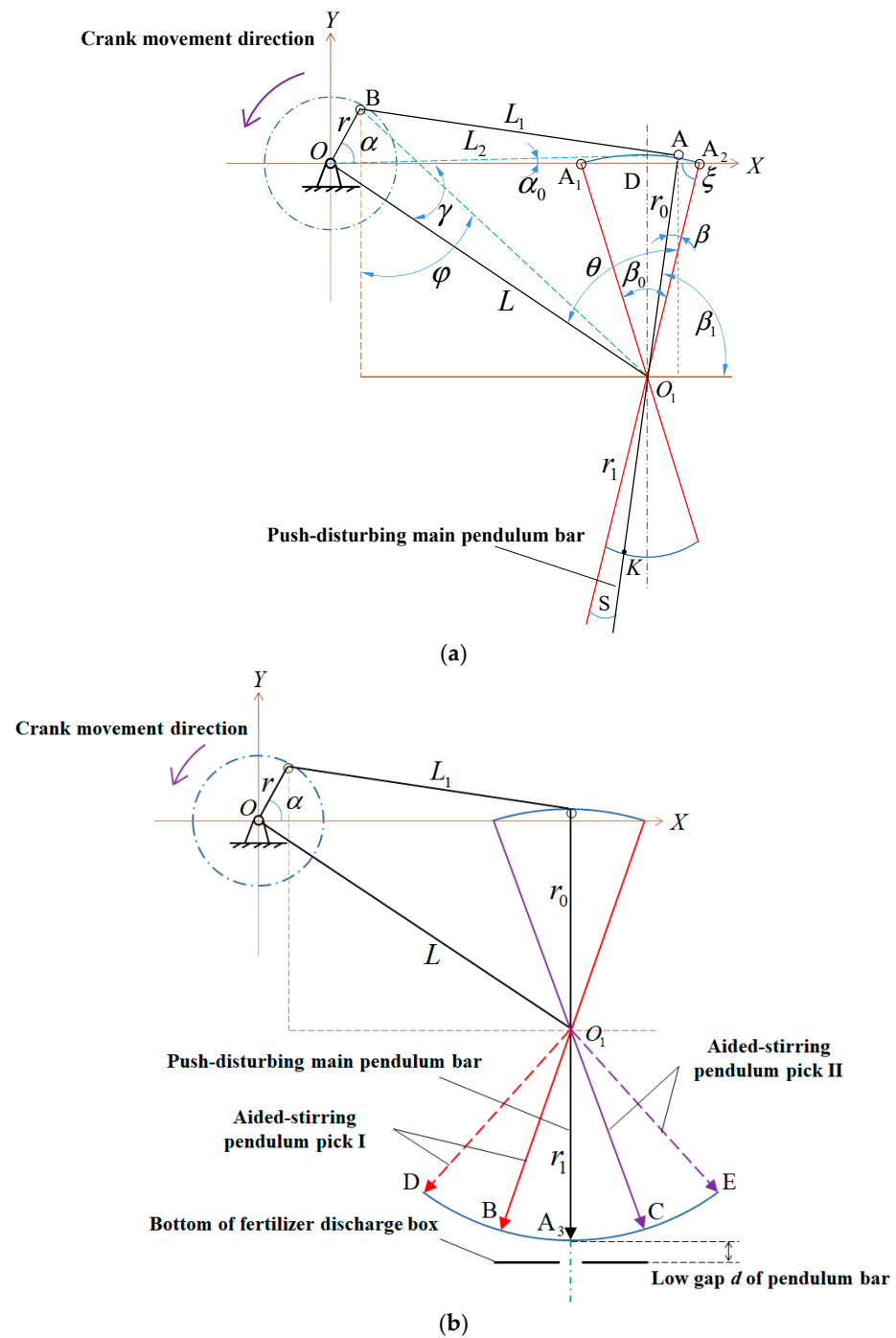


Figure 2. Schematic diagram of the combined motion analysis with swing rod combination and motion analysis of APP: (a) Schematic diagram of SRC: r , the crank radius; L_1 , the length of connecting rod; L_2 the distance between the crank rotation center O and the movement point A ; r_0 , the length of the rocker arm; r_1 , the length of main swing bar; β_0 , the swing angle; L is the distance between the crank rotation center O and the swing center O_1 ; α , the crank rotation angle; ω_0 , the crank angle velocity; β , the angular displacement of main swing bar (swing angle); α_0 , the angle between L_2 and the horizontal plane; β_1 , the angle between the main pendulum and the horizontal plane at the point of motion A ; γ , the angle between L and the horizontal; ξ , the angle between the main pendulum and the horizontal at dead center A_2 ; ω , the angular velocity of main swing bar; S , displacement of main swing rod end; V , the speed at the end of main swing bar; (b) Motion diagram of aided-stirring pendulum pick I and II. Note: B and C are the endpoint positions at the two wings of the aided-stirring pendulum pick.

2. Motion Analysis of APP

As shown in Figure 2b, the analysis indicates that the motion equation of point A_3 at the end of the main swing rod is satisfied.

$$\begin{cases} x_{A_3} = L \cos \gamma + r_1 \sin(\beta - \frac{\beta_0}{2}) \\ y_{A_3} = L \sin \gamma + r_1 \cos(\beta - \frac{\beta_0}{2}) \end{cases} \quad (10)$$

Then, the motion equations of B and C at both ends of the APP satisfy the following formula:

$$\begin{cases} x_B = L \cos \gamma + r_1 \sin(\beta - \beta_0) \\ y_B = L \sin \gamma + r_1 \cos(\beta - \beta_0) \end{cases} \quad (11)$$

$$\begin{cases} x_C = L \cos \gamma + r_1 \sin \beta \\ y_C = L \sin \gamma + r_1 \cos \beta \end{cases} \quad (12)$$

By using Equations (10)–(12), the motion equations of B and C at both ends of the APP are obtained, which are related to L , swing angle β_0 , and angular displacement β of the PMPB. The PMPB and APPs I and II are the same rigid body, and β and ω of the APP are completely the same as the PMPB. The combination motion of the SRC, the displacement, velocity, and acceleration of the PMPB, as well as the ends of APPs I and II, are sine or cosine functions of time (i.e., crank rotation angle α), and the acceleration is always proportional to the displacement. Crank rotation angle α and crank radius r determine the operating frequency f of the SRC.

The swinging frequency of the SRC is the number of times the SRC oscillates back and forth within one minute. Experiments have shown that, when the flow gap of the SRC and the size of the fertilizer discharge port are constant, the impact of the SRC on the fertilizer-discharge performance varies according to a certain pattern. With an increase in frequency, the fertilizer-discharge performance presents one of four states: unstable movement, stable fertilizer discharge, fertilizer crushing, or performance degradation. Regarding the unstable movement state, the operation frequency of the SRC is relatively low, at about 50–100 times/min. In this range, a small change in the frequency of the SRC operation will cause a significant decrease in the fertilizer-discharge performance. In the fertilizer-discharge process, when the operation frequency of the SRC is low, each swing stroke takes a long time, and in addition to the forced fertilizer discharge by the SRC, the time required for self-flow fertilizer discharge also increases relatively, resulting in an increase in discharged fertilizer. However, the pulse is large and the uniformity of fertilizer discharge is poor. Regarding the stable fertilizer-discharge state, the operation frequency of the SRC is about 100–200 times/min. Within this range, the effect of the SRC on fertilizer discharge increases with frequency, while self-flow fertilizer discharge is proportional to time and decreases with frequency. Therefore, the displacement is relatively stable, and the uniformity is also good. Regarding the fertilizer crushing and performance degradation states, the operation frequency of the SRC is greater than or equal to 200 times/min, and the fertilizer discharge rate does not change much. Due to the high frequency and the fast movement of the guide needle, the fertilizer cannot be filled in time with the SRC, resulting in a lack of material and a decrease in uniformity, which increases the fertilizer crushing index. Therefore, considering all factors, it is advisable to set the operation frequency of the SRC to 100–200 times/min. The frequency of the SRC operation should be a specific value, which is determined later through an EDEM simulation.

2.2.2. Mechanical Analysis of SRC

1. Mechanical Analysis of PMPB

The end of the PMPB is wedge-shaped and is defined as wedge angle α_1 . The amount of fertilizer discharged is affected by the following factors: the thrust F of the PMPB, the gravity mg of the fertilizer, the internal friction between the fertilizer particles, and the pressure P of the inclined plane BD. Due to the fact that a line or surface composed of any

substance only generates normal pressure on external objects when there is no friction, the friction between the wedge surface and the fertilizer can be ignored when it is smooth. For the sake of analysis, the direction of pressure P is set to be perpendicular to the BD surface, and the force analysis of the PMPB is shown in Figure 3a. When the PMPB is pushed from dead center OB to center OA_3 , the force on the fertilizer satisfies the following formula:

$$P = m \frac{dV}{dt} = mg \sin \theta - F_N f + P \cos \frac{\alpha_1}{2} \tag{13}$$

$$F_N = mg \cos \theta + P \sin \frac{\alpha_1}{2} \tag{14}$$

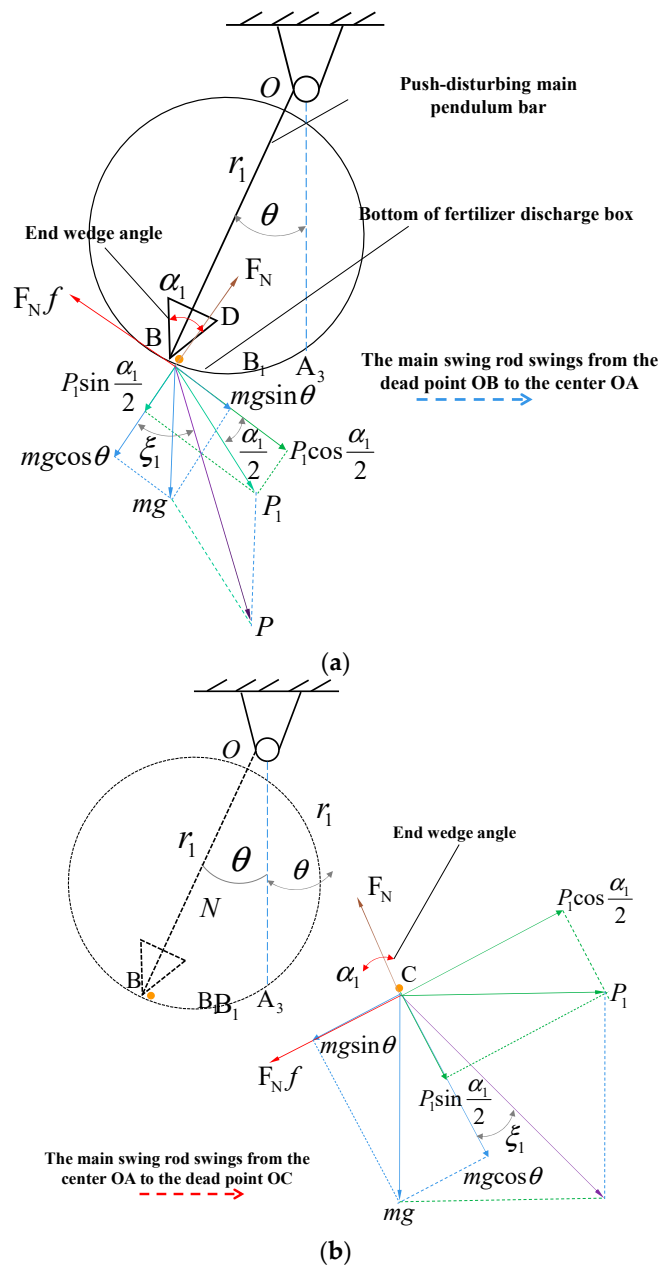


Figure 3. Schematic analysis of the dynamics of the main pendulum for pushing disturbance: (a) Schematic diagram for force analysis of main swing rod end swinging from dead point OB to center OA_3 ; (b) Schematic diagram of force analysis of main swing rod end moving from center OA_3 to dead point OC .

Simultaneous Equations (13) to (14) result in the fertilizer being subjected to inclined pressure BD.

$$P = mg \sin \theta - f(mg \cos \theta + P \sin \frac{\alpha_1}{2}) + P \cos \frac{\alpha_1}{2} \quad (15)$$

Under pressure P , the fertilizer moves along the bottom of the fertilizer box without self-locking, and the following conditions are met:

$$\zeta_1 \geq \phi_m \quad (16)$$

Here, ζ_1 is the normal angle between pressure P and the bottom of the fertilizer box ($^\circ$), and ϕ_m is the friction angle between the fertilizer and the bottom of the fertilizer box ($^\circ$).

$$\tan \zeta_1 = \frac{mg \sin \theta + P \cos \frac{\alpha_1}{2}}{mg \cos \theta + P \sin \frac{\alpha_1}{2}} \quad (17)$$

The gravity of the fertilizer is ignored, and the following formula is obtained:

$$\tan \zeta_1 = \frac{\cos \frac{\alpha_1}{2}}{\sin \frac{\alpha_1}{2}} = \cot \frac{\alpha_1}{2} \quad (18)$$

Through an analysis of SRC theory, it is determined that the friction angle is 37.5° between the fertilizer and polylactic acid (PLA) plastic. By substituting this into Equation (18), it is determined that wedge angle α_1 is 130° . The fertilizer moves along the bottom of the fertilizer box without self-locking [19] under pressure P . As shown in Figure 3b, the gravity of the fertilizer will cause fertilizer to self-lock, affecting the fertilizer discharge effect when the PMPB moves from OA_3 to dead center OC. As θ increases, the uniformity of fertilizer discharge becomes poor, so wedge angle α_1 should be smaller. In fact, to avoid particle fertilizer crushing or other debris blockage, there should be a certain gap between the tip of the guide needle and the fertilizer discharge port (swing rod flow gap). The analysis shows that the optimal wedge angle range is between 35° and 55° , and the specific values are determined later through an EDEM simulation.

2. Obliquity design of APP

APPs I and II are installed on both sides of the PMPB. The ends of APPs I and II are designed as conical surfaces for continuous fertilizer discharge, and they aim to push the fertilizers on both sides towards the center of the fertilizer discharge port. The swing centers are O_1B and O_1C , which have a phase difference from the PMPB.

During operation, both ends of APPs I and II push the fertilizer from dead point O_1D or O_1E to dead point O_1A_3 (i.e., the fertilizer discharge port), resulting in continuous fertilizer discharge. During the stages of O_1D to O_1B or O_1E to O_1C , APPs I and II are disturbed by the PMPB being pushed to discharge fertilizer. The fertilizer pushed by the APP has little effect on fertilizer discharge, except for accelerating the supplement of the fertilizer-free zone formed by the PMPB. During the stages of O_1B to O_1A_3 or O_1C to O_1A_3 , the PMPB moves toward the dead center position, pushing the fertilizer away from the discharge port, and the fertilizer pushed by the APP is discharged through the discharge port.

When the APP moves away from the fertilizer outlet, it pushes the fertilizer away from the outlet, forming a fertilizer-free zone that relies on gravity to discharge the fertilizer. MATLAB was used to illustrate the changes in the process of fertilizer discharge, which included the PMPB and APPs I and II within the working stroke. The change in the fertilizer discharge of the SRC is their superposition and synthesis, as shown in Figure 4.

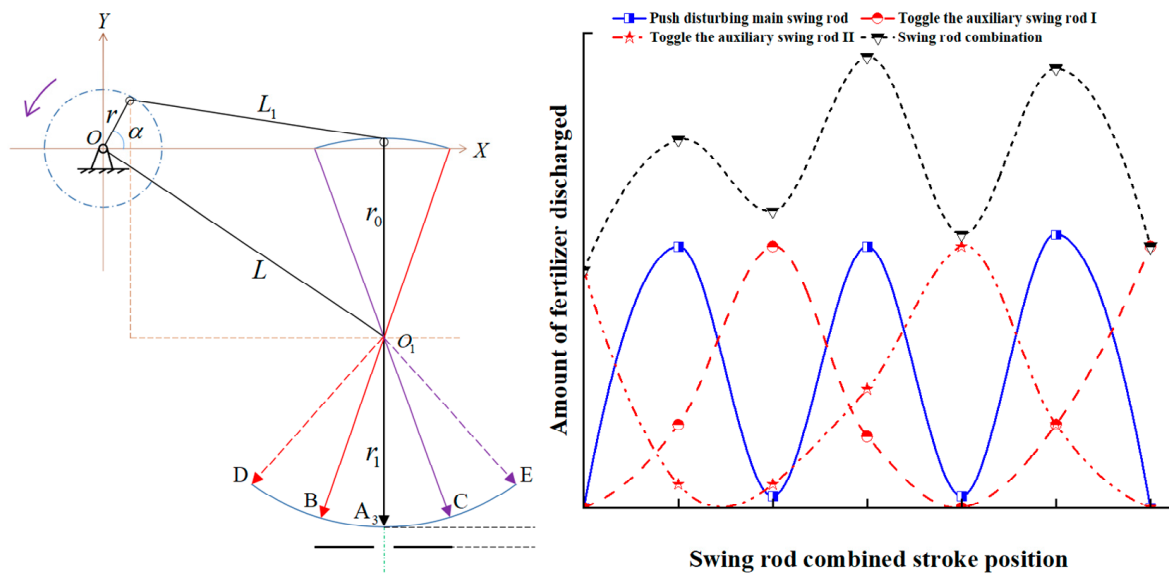


Figure 4. Variation of fertilizer discharge volume within the working stroke of the pendulum combination.

The ends of APPs I and II of the two wings are circular, and they have a backward tilt angle (δ), as shown in Figure 5. During operation, the arc can direct the fertilizer movement at each endpoint toward the fertilizer discharge port. The tilt angle has the same effect as the wedge angle designed for the end of the PMPB. Increasing the tilt angle exerts a downward movement force on the fertilizer, forcing it to move downward. Forced fertilizer discharge is beneficial for downward fertilizer discharge. Through an extensive experimental analysis in the early stage, it is determined that an inclination angle (δ) of $\sim 40\text{--}50^\circ$ is the optimal range. The specific values are determined through an EDEM simulation [20].

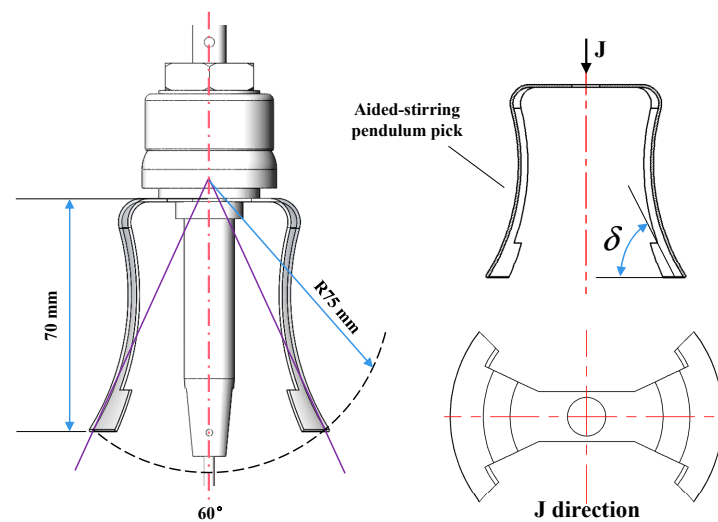


Figure 5. Schematic diagram of the structure of the aided-stirring pendulum pick.

2.2.3. Guide Needle and FGPD

The guide needle of the DFSD with a vertical pendulum bar is made of a 3 mm-diameter spring steel wire. The upper end of the guide needle is hinged to the PMPB, and the lower end is inserted into the fertilizer discharge port. As the PMPB moves, the guide needle moves up and down at the fertilizer discharge port, as shown in Figure 6.

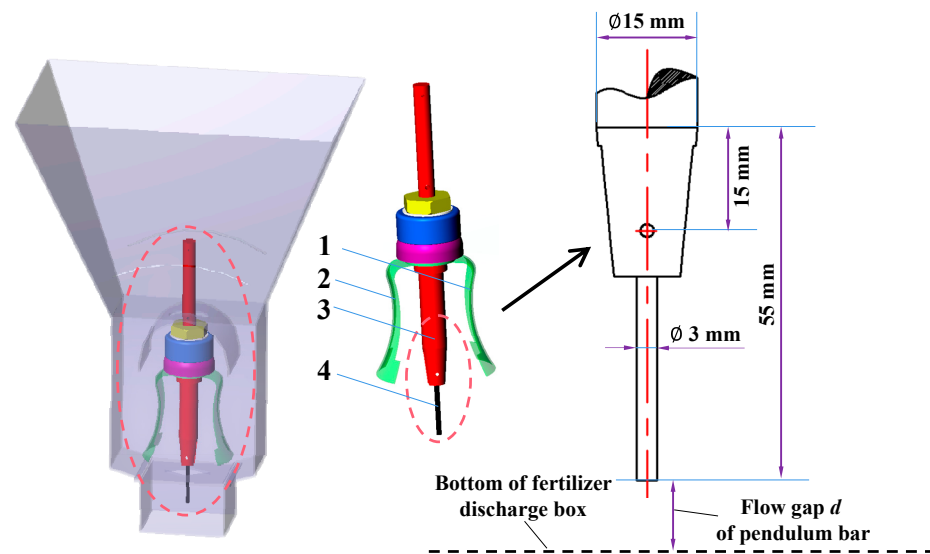


Figure 6. Schematic diagram of deflector pin structure (including FGFB): 1 Aided-stirring pendulum pick II; 2 Aided-stirring pendulum pick I; 3 Push-disturbing main pendulum bar; 4 Guide needle.

To avoid blockage in the fertilizer discharge device, the FGFB between the end of the PMPB and the bottom of the fertilizer discharge box should be considered. An experiment shows that the fertilizer discharge first increases with an increase in flow gap d under certain conditions with the operation frequency of the SRC and the size of the fertilizer discharge port. Then, the fertilizer discharge decreases with the increase in flow gap d after reaching a specific value. Obviously, the larger the flow gap d of the PMPB, the thicker the fertilizer layer between the fertilizer discharge port and the guide needle tip. The thrust of the guide needle toward the fertilizer is consumed by the friction between fertilizer particles, resulting in a smaller amount of fertilizer being pushed out of the fertilizer discharge port. To maintain a certain amount of fertilizer discharge, it is necessary to increase the fertilizer discharge port. Increasing the self-flow rate of the fertilizer will lead to a decrease in fertilizer-discharge performance. After comprehensive consideration, the optimal of the FGFB is selected as 3–8 mm, and the specific values are determined through an EDEM simulation.

2.2.4. The Amount of Fertilizer Discharged

The amount of fertilizer discharged by the DFSD depends on the SRC, the structural parameters of the guide needle, the FGFB with the PMPB, and the operating frequency of the SRC. When the FGFB and the operating frequency of the SRC are within a certain range, the fertilizer discharge Q (g/time) caused by the SRC swinging back and forth remains almost unchanged [19], and the calculation is based on the following formula:

$$Q = \frac{5Q_1 B v_m}{3f m} \quad (19)$$

In the formula, Q_1 is the fertilizer discharge per unit area required by agricultural technology, kg/hm^2 ; B is the working width of the fertilizer applicator, m ; v_m is the operating speed of the fertilizer applicator, km/h ; and m is the number of fertilizer discharge devices.

In summary, the main factors that affect the performance of the DFSD with a vertical pendulum bar are the wedge angle α_1 of the PMPB, the tilt angle δ of the APP, the FGFB of the PMPB, and the operation frequency f of the SRC.

2.3. Simulation Test

2.3.1. Simulation Model Establishment

The discrete element method (DEM) treats a simulated medium system as a set of particles with a certain shape and mass, and it represents mechanical components with boundary walls. Different physical properties and interaction relationships between the simulated medium and working components are considered, and then certain initial conditions are provided by assigning specific contact models and parameters between particles and between particles and boundaries. This allows for the use of energy exchange to predict the motion of particle groups [21], which is generated by the collision between particles and boundaries. To predict the motion of each single particle, the motion of each single particle is tracked. Supposing that the fertilizer discharge process occurs in an ideal anhydrous environment, the Hertz–Mindlin non-sliding contact model was selected as the contact model between particles and the geometry of the fertilizer discharge device [22], as shown in Figure 7.

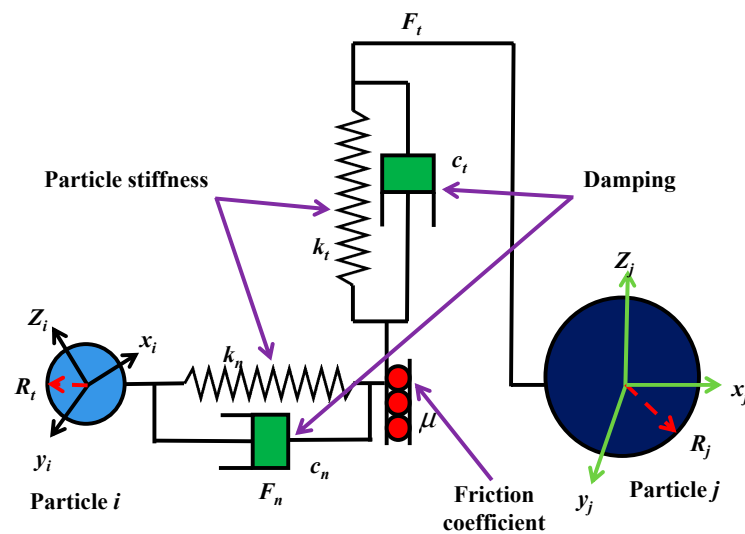


Figure 7. Hertz–Mindlin (no slip) contact model.

This study used fertilizer 30-5-5 as the experimental object, which is produced by Akon Company in Russia. First, 200 fertilizer particles were randomly selected from a pile, and three-axis dimensions of the fertilizer were measured. Finally, the calculated equivalent diameter was 3.5 mm, and the spherical index was 94.88%.

$$D_K = \sqrt[3]{L_K W_K H_K} \tag{20}$$

$$\varphi_K = \frac{D_K}{L_K} \tag{21}$$

In the equation, D_k is the equivalent diameter, m; φ_k is the spherical index, %; and L_k , W_k , and H_k are the three axis dimensions of the fertilizer, m.

The spherical index of the fertilizer has exceeded 90% after measurement and calculation, indicating that the particles in this batch of samples have high spherical distribution characteristics. Therefore, it was determined to be appropriate to choose a sphere with a diameter of 3.5 mm as the simulation model. The normal distribution function of Equation (22) was used to fit the sample distribution pattern data.

$$y = y_a + ke^{-\frac{(x-x_0)^2}{2b^2}} \tag{22}$$

In the equation, y is the dependent variable, x is the independent variable, and y_a , k , x_0 , and b are the coefficients of the normal distribution function. The particles had a fitting

degree of $R^2 = 0.98$. Thus, it could be considered that the equivalent diameter of the particles followed the normal distribution law. Therefore, it was determined that the production law of the fertilizer particles in the particle factory followed a normal distribution, as shown in Figure 8.

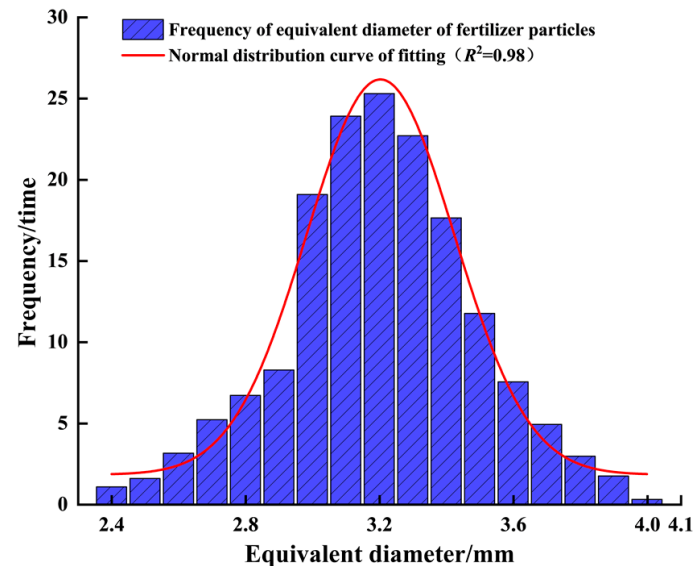


Figure 8. Equivalent diameter and grain-size distribution of fertilizers.

By consulting Reference [23] and conducting fertilizer parameter-calibration experiments, the fertilizer discharge device was 3D printed with PLA plastic. The simulation parameters are shown in Table 1, and the simulation parameters of the particles and models are shown in Table 2.

Table 1. Basic parameters set of EDEM.

Project	Parameter	Unit	Values
Fertilizer granules	Poisson's ratio	/	0.25
	Shear modulus	pa	2.6×10^7
	Density	kg/m ³	1861
Fertilizer-discharge box and swing rod combination	Poisson's ratio	/	0.394
	Shear modulus	pa	1.3×10^9
	Density	kg/m ³	1240
Fertilizer granules and fertilizer granules	Restitution	/	0.11
	Static friction coefficient	/	0.30
	Rolling friction coefficient	/	0.10
Fertilizer granules, fertilizer-discharge box, and swing-rod combination	Restitution	/	0.41
	Static friction coefficient	/	0.32
	Rolling friction coefficient	/	0.18

Table 2. Parameter set of EDEM simulation.

Parameter	Unit	Value
Time step	s	9.25×10^{-6}
Acceleration	m·s ⁻²	0
Stiffness and damping coefficient	/	0
Local damping coefficient	/	0

As shown in Figure 9, a fertilizer-collection belt, with a length of 1000 mm and a width of 100 mm, is placed below the fertilizer discharge port to observe the distribution

of the fertilizer after discharge. A simulation box particle factory is placed on top of the fertilizer-discharge device, generating a total of 40,000 particles. The command of the Add Sinusoidal Rotation Kinematic in the Add Motion module is applied to the PMPB, APP, and guide needle swing. The overall linear movement of the fertilizer-discharge device can be achieved by applying the command of the Add Linear Translation Kinematic. The forward speed is set to 0.5 m/s, 20% of the step size is taken as the simulation time step for the Rayleigh time of EDEM, and the simulation time is 14 s. Using EDEM post-processing to obtain the velocity change curve and motion trajectory of each particle, the force data of the SRC are derived during the fertilizer movement process at three positions in the disturbed and fallen fertilizer areas during the simulation time.

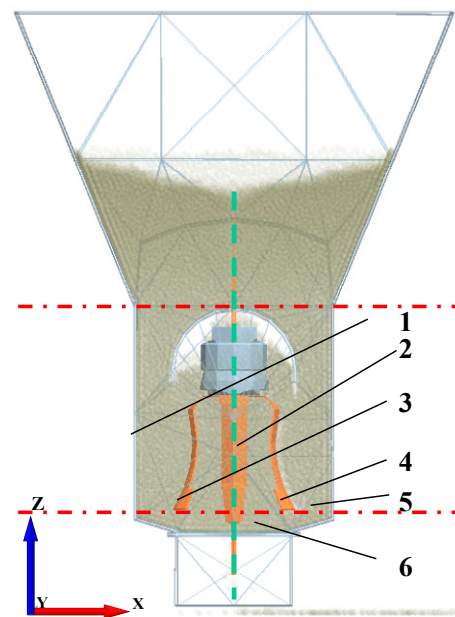


Figure 9. Discrete element-simulation process of disturbed fertilizer strip-ejection device with vertical pendulum bar: 1 Area I; 2 Push-disturbing main pendulum bar; 3 Aided-stirring pendulum pick I; 4 Aided-stirring pendulum pick II; 5 Area II; 6. Area III.

2.3.2. Analysis of Discrete Element Simulation Process

EDEM post-processing was used to show the velocity of the fertilizer group in color, marking the movement trajectory and velocity changes in the fertilizer during the fertilizer discharge process. Figure 10 shows a distribution map of the fertilizer movement simulation speed, where red represents the fastest speed, blue represents the slowest speed, and the direction of the black dashed arrow represents the direction of the fastest particle group velocity.

When the SRC of the fertilizer-discharge device starts to move, the SRC moves left from the center position. Due to the squeezing of fertilizer and the movement of the SRC, the flow direction of the particle group is concentrated in the right area of the SRC at a faster speed, as shown in Figure 10b. When the SRC moves from the left area to the center, it is subjected to the gravity of the fertilizer particles and the compression between the particles. The flow direction of the particle group is mainly distributed in the left area of the SRC, as shown in Figure 10c. When the SRC moves from the center to the right, the speed of the particle group is significantly increased. Due to the squeezing of the fertilizer and the collision motion of the SRC, the flow direction of the particle group is concentrated on the left side of the SRC. The red area is large, as shown in Figure 10d. When the SRC moves from the right area to the center, it is subjected to the gravity of the fertilizer and the squeezing effect between the particles. The particle group flows towards the positions on both sides of the SRC, and the speed is relatively high, as shown in Figure 10e. This completes one motion cycle of the SRC. The fertilizer removal effect is shown in Figure 10f.

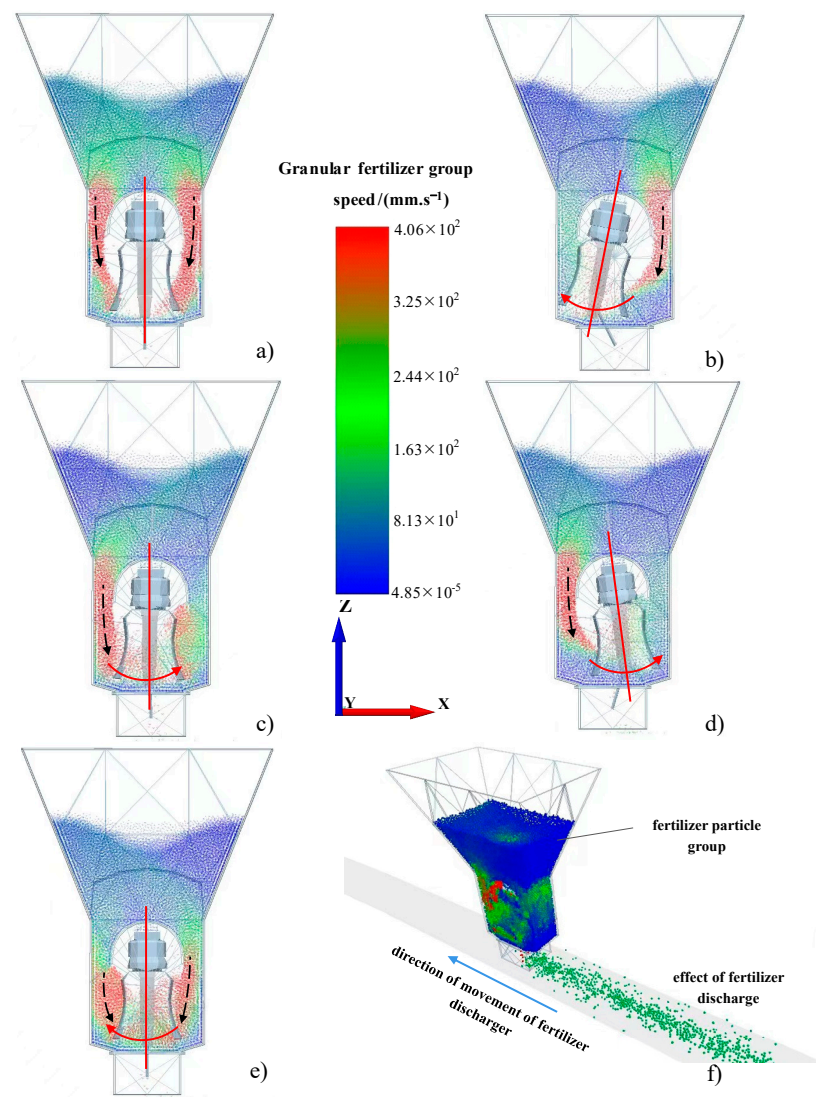


Figure 10. Simulation results of fertilizer particle movement: (a) Swing rod combination is stationary; (b) Swing rod assembly moves from center to left; (c) The swing bar assembly moves from the left area to the center; (d) The swing bar assembly moves from the center to the right; (e) The swing bar assembly moves from the right area to the center; (f) The fertilizer removal effect.

To analyze the stress situation of key components in the fertilizer box, the force data of Sensor 1 in Zone I, Sensor 2 in Zone II, and Sensor 3 in Zone III, which monitor the fertilizer box, are exported, as shown in Figure 11. The average total force on the fertilizer box measure by Sensors 1, 2, and 3 is 35.32 N, 34.98 N, and 26.68 N. To further investigate the movement mechanism of the fertilizer in the fertilizer discharge device, three fertilizers were randomly selected from the fertilizer box. As shown in Figure 11b, the average particle velocity curve was exported using the Geometry Bin, which was applied under the Setup Selections module. Regarding the first fertilizer, when it falls into the fertilizer discharge-movement zone within $\sim 0\text{--}4$ s, the fertilizer particles are in a fluctuating state, and the speed significantly increases. Under the disturbance of the SRC, the particles are subjected to collisions with other particles and the SRC, resulting in significant fluctuations in velocity, which reaches a peak at $\sim 4\text{--}9.5$ s. At $\sim 9.5\text{--}12$ s, the particles move to the fertilizer-discharge outlet and are subjected to the action of the guide needle, resulting in a significant change in particle velocity. When the fertilizer leaves the discharge port after 12 s, the velocity rapidly drops to 0, completing the fertilizer-discharge process. Under the disturbance of the pendulum combination, the second fertilizer reaches its peak speed at $\sim 8\text{--}11$ s. The speed

of the third fertilizer fluctuates significantly and reaches its peak under the disturbance of the SRC at ~3–9 s. The particles are subjected to the action of the guiding needle, resulting in a significant change in velocity at ~9–12 s.

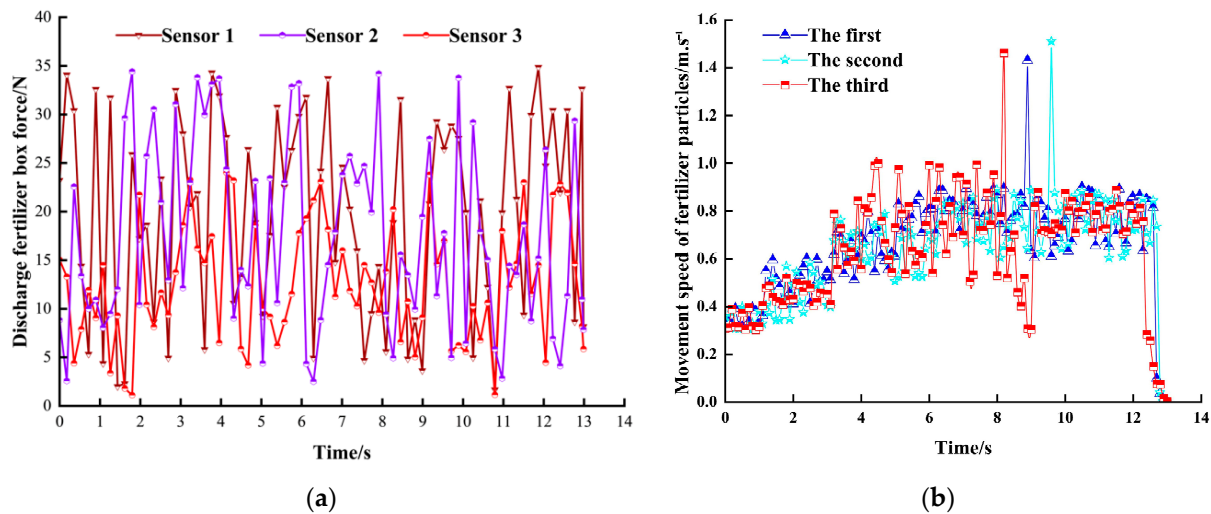


Figure 11. Analysis of fertilizer-particle simulation results: (a) Discharge fertilizer tank force change curve; (b) Velocity versus time curve of granular fertilizer movement.

2.3.3. Experimental Factors and Levels

Through extensive experiments in the early stage, it was found that the wedge angle of the PMPB was ~35–55°, the inclination angle of the APP was ~40–50°, the operation frequency of the SRC was ~100–200 times/min, and the FGPB was ~3–8 mm. To obtain the optimal parameter combination, a four-factor and five-level orthogonal center combination test method was selected for simulation research, as shown in Table 3.

Table 3. Test factors and levels.

Levels	Wedge Angle of PMPB $X_1/(\circ)$	Inclination Angle of APP $X_2/(\circ)$	Operating Frequency of SRC $X_3/(\text{times}/\text{min})$	FGPB X_4/mm
−2	35.00	40.00	100.00	3.00
−1	40.00	42.50	125.00	4.25
0	45.00	45.00	150.00	5.50
1	50.00	47.50	175.00	6.75
2	55.00	50.00	200.00	8.00

2.3.4. Calculation of Evaluation Indicators

The coefficient of variation (CV) Y_1 and fertilizer discharge accuracy (FDA) Y_2 [24] were used to evaluate the uniformity of fertilizer discharge and stability during the process. The grid method was used to obtain data statistics on the uniformity of fertilizer discharge [4,25]. According to the forward speed of the fertilizer discharge device, the collected fertilizer strips were divided into five repeated test zones with a length of 1000 mm along the x-axis. Each zone was subdivided using eight statistical grids with a length and width of 125 mm and 100 mm, and the fertilizer quality within the eight grids was calculated. The statistical grid settings are shown in Figure 12.

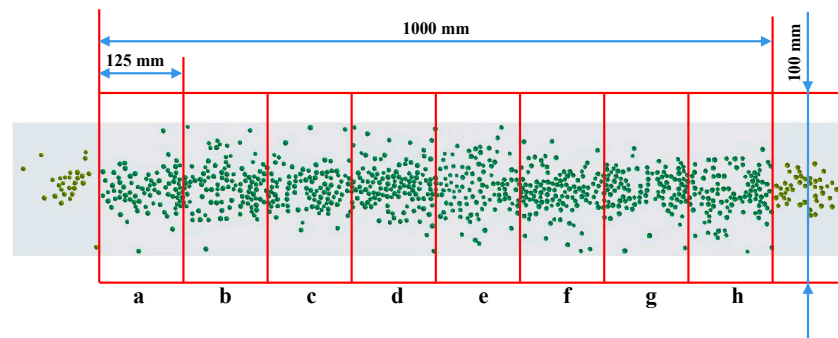


Figure 12. Grid settings diagram. Note: The 8 statistical grids in each cell are numbered as a~h in the positive region.

The fertilizer discharge performance of this group was calculated using Equations (23)–(25), and the average fertilizer discharge quality, standard deviation, and CV Y_1 of fertilizer uniformity were obtained in the grid unit [4,18].

$$\bar{m} = \sqrt{\frac{\sum_{i=1}^8 m_i}{n}} \quad (i = 1, 2, \dots, 8) \quad (23)$$

$$s = \sqrt{\frac{\sum_{i=1}^8 (m_i - \bar{m})^2}{n - 1}} \quad (i = 1, 2, \dots, 8) \quad (24)$$

$$Y_1 = \frac{s}{\bar{m}} \times 100\% \quad (25)$$

In the formula, m_i represents the total mass of the fertilizer particles in grid i , g ; n indicates the number of statistical grid cells, $n = 8$; \bar{m} represents the average mass of the fertilizer particles in the statistical grid unit, g ; S represents the standard deviation between each statistical grid unit in a single experiment, g ; and Y_1 represents the CV of fertilizer uniformity between each statistical grid unit in a single experiment, %. The smaller the CV of the fertilizer-discharge uniformity between each statistical grid unit, the better the stability and uniformity of the fertilizer discharge of the fertilizer discharge device. Therefore, the CV of the fertilizer discharge uniformity between each statistical grid unit is used as an evaluation indicator to analyze the operational performance of the fertilizer discharge devices under different structural parameters.

FDA Y_2 represents the difference between the theoretical and actual fertilization amounts. The higher the FDA, the smaller the deviation of the fertilizer discharge [26]. The fertilizer-discharge quality within a single fertilizer discharge cycle was measured, and it was compared with the theoretical value. This was repeated three times to calculate the FDA.

2.4. Test Materials and Equipment

To verify the accuracy of the simulation and the rationality of the prototype design, a trial production fertilizer-discharge device test bench was developed for verification. The experiment was conducted at the Mechanical Engineering Laboratory of Guangxi Normal University at Yucai Guilin of Guangxi Autonomous Region, between 26 May and 27 May 2023.

In the experiment, fertilizer 30-5-5 was used as the experimental material, consistent with the simulation. The wedge angle of the PMPB was set to 45° , the inclination angle of the APP was set to 46° , the operation frequency of the SRC was 188 times/min, and the FGPB was 4.5 mm. The fertilizer discharge device was fixed on a rack. The instruments used included not only an electronic scale, with a weighing range of 30 kg and an accuracy of

0.01 g, but also a switching power supply, a plastic basin for moisture content measurement, and a timer.

In the experiment, a certain amount of fertilizer that exceeded two-thirds of the capacity of the fertilizer box was loaded into the fertilizer box [27,28], and the operation frequency of the SRC was adjusted. The experimental data were collected in several steps: First, data on the fertilizer quality were collected in real time through a serial port connected to a computer based on the electronic scale. Second, the data collection interval was set to 250 ms, and the fertilizer output during each combined swing movement cycle was recorded eight times in chronological order. The CV was calculated between eight data points during the period of the combined swing motion. To reduce experimental pulsation interference and obtain accurate results, the experiment was repeated five times, and the average of the results was taken (Figure 13).

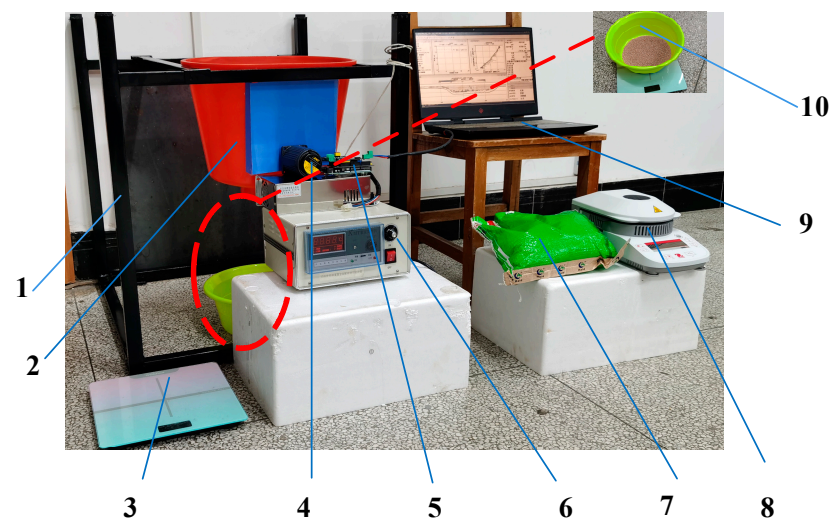


Figure 13. Bench test: 1 Frame; 2 Fertilizer discharge device; 3 Electronic scale; 4 Motor 5 Power supply serial port; 6 Electronic speed controller; 7 Fertilizer; 8 Moisture content detector; 9 Data-acquisition interface; 10 Plastic basin.

3. Results

3.1. Results of Regression Model

3.1.1. Scheme and Results of the Experiment

The experimental plan and results are shown in Table 4. Each group of experiments was repeated three times, and the average of the experimental results was taken.

Table 4. Experiment scheme and results.

Test No.	Experimental Factors				Test Index	
	$x_1/(^\circ)$	$x_2/(^\circ)$	$x_3/(\text{times}/\text{min})$	x_4/mm	$Y_1/\%$	$Y_2/\%$
1	−1	−1	−1	−1	6.50	1.56
2	1	−1	−1	−1	19.92	4.86
3	−1	1	−1	−1	24.16	5.85
4	1	1	−1	−1	23.41	5.52
5	−1	−1	1	−1	14.71	3.28
6	1	−1	1	−1	11.61	3.22
7	−1	1	1	−1	17.04	4.42
8	1	1	1	−1	14.70	3.84
9	−1	−1	−1	1	17.59	4.20

Table 4. Cont.

Test No.	Experimental Factors				Test Index	
	$x_1/(\text{°})$	$x_2/(\text{°})$	$x_3/(\text{times/min})$	x_4/mm	$Y_1/\%$	$Y_2/\%$
10	1	−1	−1	1	29.00	5.85
11	−1	1	−1	1	20.36	4.19
12	1	1	−1	1	25.82	5.45
13	−1	−1	1	1	22.72	5.31
14	1	−1	1	1	19.09	4.73
15	−1	1	1	1	16.04	4.20
16	1	1	1	1	11.61	3.22
17	−2	0	0	0	23.89	5.19
18	2	0	0	0	33.41	7.16
19	0	−2	0	0	12.40	2.92
20	0	2	0	0	21.01	4.03
21	0	0	−2	0	25.97	5.30
22	0	0	2	0	15.35	3.62
23	0	0	0	−2	8.21	2.19
24	0	0	0	2	19.13	3.80
25	0	0	0	0	31.73	7.17
26	0	0	0	0	30.29	6.84
27	0	0	0	0	31.73	7.17
28	0	0	0	0	27.41	6.18
29	0	0	0	0	31.73	7.17
30	0	0	0	0	27.41	6.18
31	0	0	0	0	30.29	6.84
32	0	0	0	0	32.41	7.56
33	0	0	0	0	30.73	7.17
34	0	0	0	0	32.41	7.56
35	0	0	0	0	30.29	6.84
36	0	0	0	0	30.73	7.17

3.1.2. Regression Model and Significance Test 2

An analysis of variance of the experimental results is shown in Table 5.

Table 5. Regression analysis of Y_1 and Y_2 .

Index	Source	Sum of Squares	Freedom	F	p
Y_1	Model	1982.12	11	34.21	<0.0001 **
	x_1	51.28	1	9.74	0.0047 **
	x_2	35.58	1	6.75	0.0157 *
	x_3	152.41	1	28.94	<0.0001 **
	x_4	112.75	1	21.41	0.0001 **
	x_1x_2	25.4	1	4.82	0.038 *
	x_1x_3	115.78	1	21.98	<0.0001 **
	x_2x_3	54.32	1	10.31	0.0037 **
	x_2x_4	105.78	1	20.08	0.0002 **
	x_2^2	444.67	1	84.43	<0.0001 **
	x_3^2	240.06	1	45.58	<0.0001 **
	x_4^2	644.11	1	122.3	<0.0001 **
	Residual	126.4	24		
	Lack of fit	95.35	13	2.6	0.0606
Error	31.06	11			
Sum	2108.53	35			

Table 5. Cont.

Index	Source	Sum of Squares	Freedom	F	p
Y ₂	Model	91.23	12	36.12	<0.0001 **
	x ₁	2.42	1	11.49	0.0025 **
	x ₂	1.45	1	6.89	0.0151 *
	x ₃	3.1	1	14.71	0.0008 **
	x ₄	2.55	1	12.11	0.002 **
	x ₁ x ₂	1.53	1	7.25	0.013 *
	x ₁ x ₃	4.08	1	19.39	0.0002 **
	x ₂ x ₃	1.82	1	8.66	0.0073 **
	x ₂ x ₄	5.93	1	28.17	<0.0001 **
	x ₁ ²	1.15	1	5.48	0.0283 *
	x ₂ ²	23.93	1	113.7	<0.0001 **
	x ₃ ²	12.24	1	58.17	<0.0001 **
	x ₄ ²	31.03	1	147.45	<0.0001 **
	Residual	4.84	23		
	Lack of fit	2.65	12	1.11	0.4358
Error	2.19	11			
Sum	96.07	35			

Note: x₁, x₂, x₃ and x₄ are the level values of X₁, X₂, X₃, X₄. * indicates significant difference (p < 0.05), ** indicates highly significant difference (p < 0.01).

Design expert software was used to perform a multiple regression fitting analysis on the results in Table 4, and regression equations were established for Y₁ and Y₂ with x₁, x₂, x₃, and x₄.

$$Y_1 = 30.1 + 1.46x_1 + 1.22x_2 - 2.52x_3 + 2.17x_4 - 1.26x_1x_2 - 2.69x_1x_3 - 1.84x_2x_3 - 2.57x_2x_4 - 3.73x_2^2 - 2.74x_3^2 - 4.49x_4^2 \quad (26)$$

$$Y_2 = 6.99 + 0.3175x_1 + 0.2458x_2 - 0.3592x_3 + 0.3258x_4 - 0.3088x_1x_2 - 0.5050x_1x_3 - 0.3375x_2x_3 - 0.6087x_2x_4 - 0.1898x_1^2 - 0.8648x_2^2 - 0.6185x_3^2 - 0.9848x_4^2 \quad (27)$$

According to the analysis in Table 5, the CV Y₁ of fertilizer uniformity and the regression model of FDA Y₂ are extremely significant (p < 0.01). Specifically, the CV of fertilizer uniformity F is equal to 34.21, and p is less than 0.001; the FDA of F is equal to 36.12, and p is less than 0.001. The CV of fertilizer uniformity Y₁ and the loss of fit term in the regression model of FDA Y₂ are not significant (p > 0.05). Specifically, the CV of fertilizer uniformity F₂ is equal to 2.6, and P₂ is equal to 0.0606; the CV of vertical fertilizer uniformity F₂ is equal to 1.11, and P₂ is equal to 0.4358. This proves that the CV of uniformity Y₁ and FDA Y₂ have good fitting effects, and there are no other main factors affecting the indicators. For the CV of fertilizer uniformity Y₁, x₁, x₃, x₄, x₁x₃, x₂x₃, x₂x₄, x₂², x₃², and x₄² have a very significant impact (p < 0.01), while x₂ and x₁x₂ have a significant impact (0.01 < p < 0.05). For FDA Y₂, x₁, x₃, x₄, x₁x₃, x₂x₃, x₂x₄, x₂², x₃², and x₄² have a significant impact (p < 0.01), while x₂, x₁x₂, and x₁² have a significant impact (0.01 < p < 0.05). The analysis shows that the sequence of factors affecting the CV and FDA is the operation frequency of the SRC, the FGPB, the wedge angle of the PMPB, and the inclination angle of the APP.

3.2. Analysis of Simulation Results of Key Component

3.2.1. Analysis of Factors Influencing Effects

The response surface of factors to evaluation indicators is examined. As shown in Figure 14a, with the increase in the wedge angle α₁ of the PMPB, CV Y₁ first increases, then reaches a peak, and finally remains flat. When the wedge angle α₁ of the PMPB reaches 45°, CV Y₁ reaches a peak. With the increase in the inclination angle δ of the APP, the CV of uniformity first increases and then decreases. When the inclination angle of the APP is ~44.5–46.5°, the CV of uniformity reaches its optimal value.

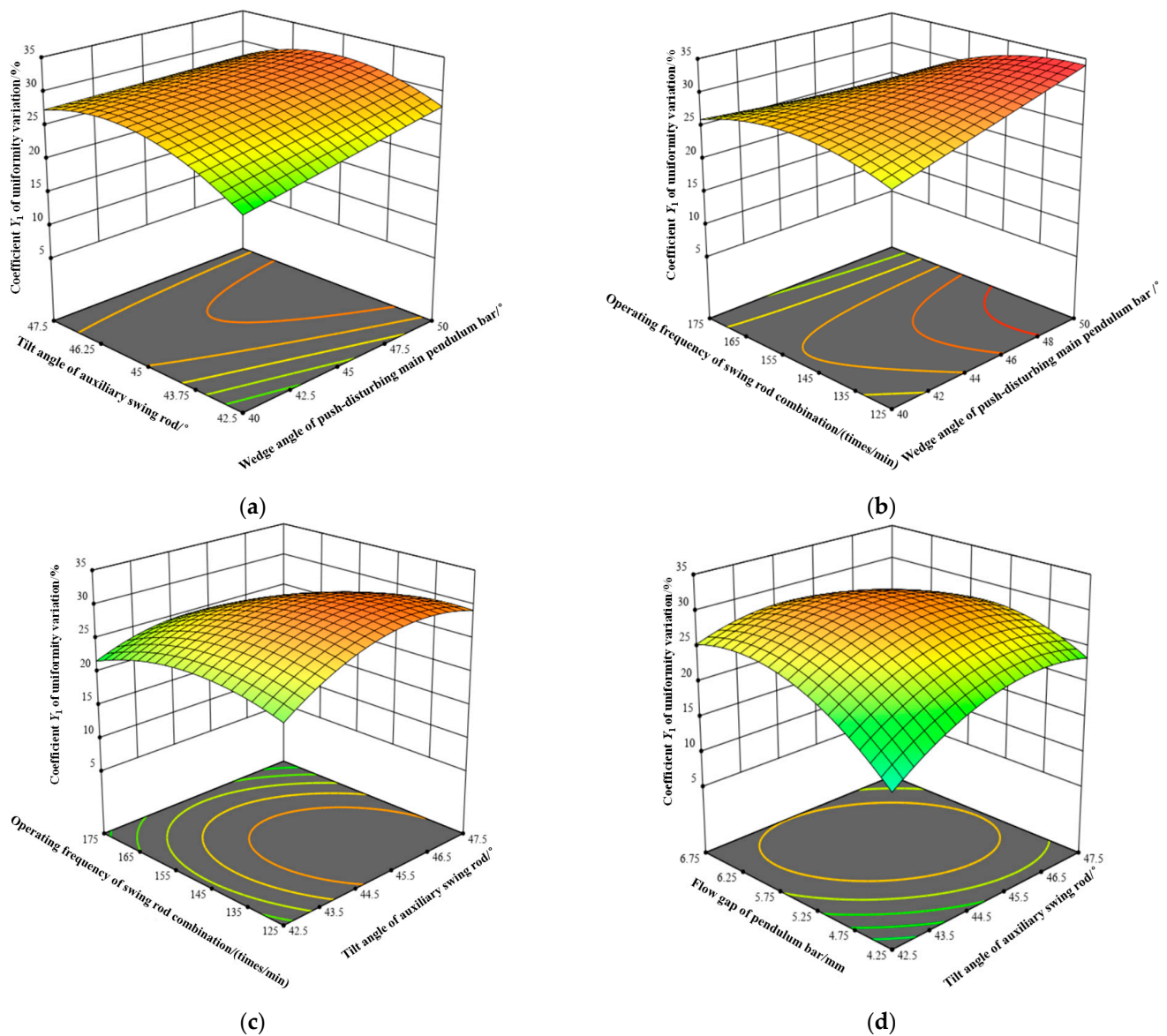


Figure 14. The influence rule of each test factor on the CV of uniformity: (a) $Y_1 = f(X_1, X_2, 0, 0)$; (b) $Y_1 = f(X_1, 0, X_3, 0)$; (c) $Y_1 = f(0, X_2, X_3, 0)$; (d) $Y_1 = f(0, X_2, 0, X_4)$.

As shown in Figure 14b, the CV of uniformity decreases as the operation frequency of the SRC increases. When the operation frequency of the SRC is ~125–145 times per minute, the CV of uniformity reaches its optimal value. When the wedge angle of the PMPB increases with the push disturbance, the CV of uniformity increases. When the wedge angle of the PMPB reaches 48° , the CV of uniformity reaches its peak.

As shown in Figure 14c, as the operation frequency of the SRC increases, the CV of uniformity decreases. When the operation frequency of the SRC increases from 125 to 155 times per minute, the optimal value is achieved. When the inclination angle of the APP increases, the CV of uniformity first increases, then reaches its peak and remains flat. When the inclination angle of the APP reaches 44.5° , the CV of uniformity reaches its peak.

As shown in Figure 14d, as the FGPB increases, the CV of uniformity first increases, reaches its peak, and then slowly decreases. When the FGPB is 5.25 mm, the CV of uniformity reaches its optimal value. When the inclination angle of the APP increases, the CV of uniformity first increases. Then it reaches its peak and finally slowly decreases. When the tilt angle value of the APP is ~42–47°, the CV of uniformity reaches the optimal value.

As shown in Figure 15a, the FDA first increases with the increase in the wedge angle of the PMPB then reaches its peak and finally shows a gentle and unchanging trend. When the wedge angle of the PMPB is ~42–50°, the FDA reaches the optimal value. When the inclination angle of the APP increases, the FDA shows a trend of gradually increasing until it reaches the peak and then slowly decreasing. When the inclination angle of the APP reaches 43.5°, the FDA reaches the peak.

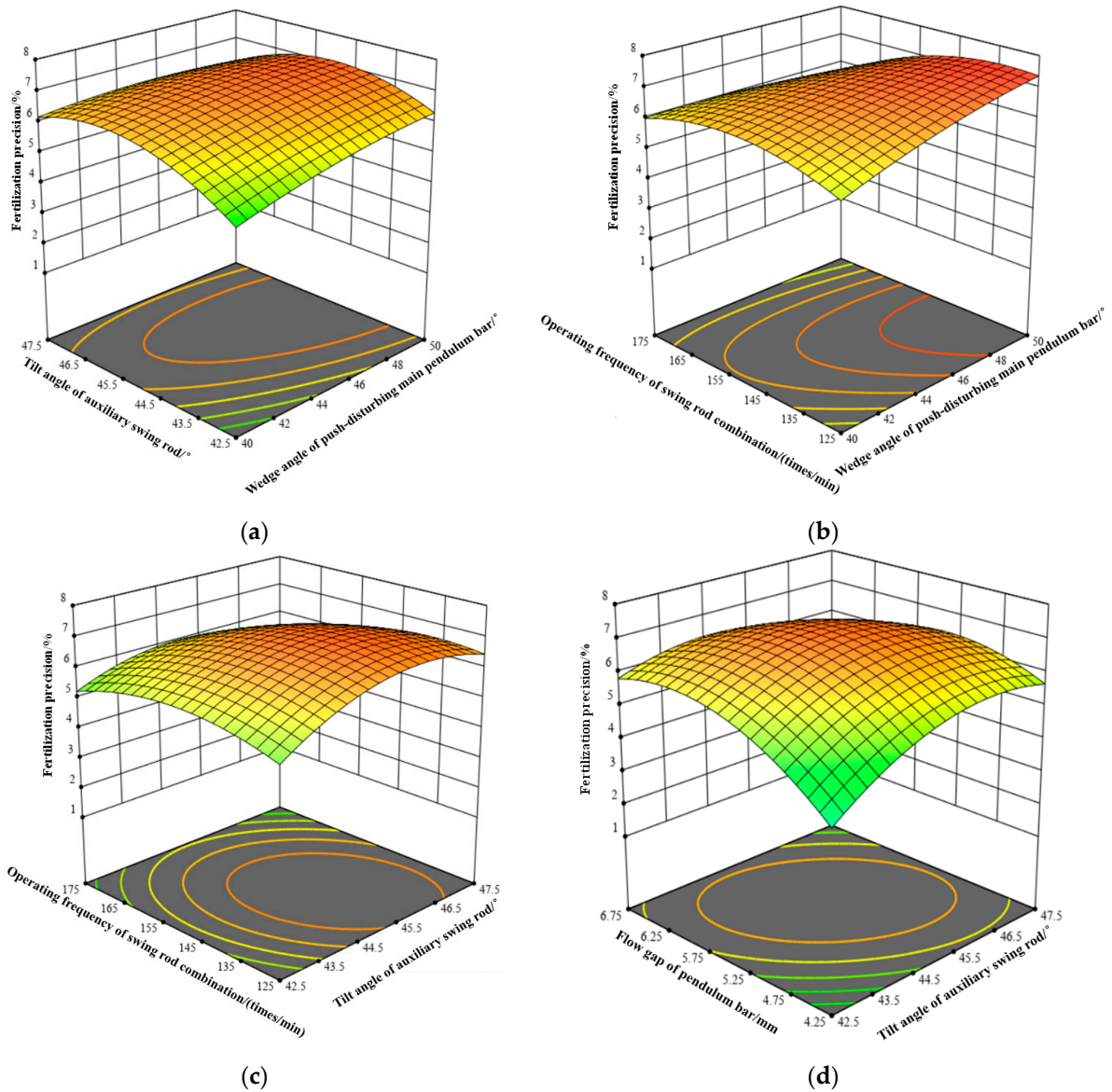


Figure 15. The influence rule of various experimental factors on fertilization accuracy: (a) $Y_2 = f(X_1, X_2, 0, 0)$; (b) $Y_2 = f(X_1, 0, X_3, 0)$; (c) $Y_2 = f(0, X_2, X_3, 0)$; (d) $Y_2 = f(0, X_2, 0, X_4)$.

As shown in Figure 15b, as the operation frequency of the SRC increases, the FDA decreases. When the operation frequency of the SRC is 125-to-145 times per minute, the FDA reaches the optimal value. When the wedge angle of the PMPB increases, the FDA decreases. When the wedge angle of the PMPB reaches 47°, the FDA reaches its peak.

As shown in Figure 15c, as the operation frequency of the SRC increases, the FDA increases. When the operation frequency of the SRC is 125-to-155 times per minute, the optimal value is reached. When the inclination angle of the APP increases, the FDA first increases, then reaches its peak, and finally shows a slow downward trend. When the inclination angle of the APP reaches 44.5°, the FDA reaches its peak.

As shown in Figure 15d, as the FGPB increases, the FDA first increases then reaches its peak before finally showing a slow downward trend. When the FGPB is 5.25-to-6.50 mm, the FDA reaches its optimal level. When the inclination angle of the APP increases, the FDA first increases, then it reaches its peak and finally slowly decreases. When the tilt angle value of the APP is $\sim 42\text{--}47^\circ$, the FDA reaches the optimal value.

3.2.2. Optimization of Key Component Parameters

Based on the range of values for each factor, the objective function and constraint conditions are as follows:

$$\begin{cases} Y_1 \leq 10\% \\ Y_2 \leq 5\% \\ 35^\circ \leq X_1 \leq 55^\circ \\ 40^\circ \leq X_2 \leq 50^\circ \\ 100 \leq X_3 \leq 200 \\ 3 \leq X_4 \leq 8 \end{cases} \quad (28)$$

The optimal parameters were solved using the Optimization module in Design Expert 13 software, the wedge angle of the PMPB was 45.65° , the inclination angle of the APP was 46.86° , the operating frequency of the SRC was 187.85 times per minute, and the FGPB was 4.50 mm. The model predicted that the CV of fertilizer uniformity would be 10% and that the FDA would be 3.09%. After rounding, the wedge angle of the PMPB was 45° , the inclination angle of the APP was 46° , the operation frequency of SRC was 188 times per minute, and the FGPB was 4.50 mm. The model predicted a CV of 10.53% and an FDA of 3.19%.

3.3. Bench Test Results

3.3.1. Test Results

The bench validation test results are shown in Table 6, which also shows the calculated CV and FDA of the actual fertilizer. The CV of fertilizer uniformity was 11.06% and the FDA was 3.51%. Compared to the results of the simulation tests, the CV of fertilizer uniformity was 10.53% and the FDA was 3.19%. There was a certain deviation between the results of the simulation tests and the bench-validation tests. A reason for the deviation is that, in the simulation, the individual fertilizer particles established were not standard spheres, and the dispersion degree of the particle groups was not a completely normal distribution. However, in the actual bench tests, the uniformity and dispersion degree of the fertilizers used were relatively poor, so the CV obtained from the bench validation tests was slightly higher than the CV obtained from the simulation tests. Therefore, it can be considered that the simulation results are basically consistent with the measured results.

Table 6. Bench test results.

No.	$Y_1/\%$	$Y_2/\%$
1	10.71	3.45
2	11.89	3.77
3	11.42	4.18
4	10.53	2.98
5	10.77	3.17
average value	11.06	3.51

3.3.2. Results of Fertilizer Discharge Performance Tests at Different Frequencies

In order to further analyze the fertilizer discharge performance of the spiral fertilizer applicator, the fertilizer discharge performance of the fertilizer applicator was tested at a gradient of 20 times/min within the operating frequency range of 100–200 times/min (the optimal operating frequency range). The other experimental indicators were the same as those in the bench test, and the average value was taken for each group of experiments

repeated five times. The calculation of the bench test data is shown in Table 7. It can be seen that the CV of uniformity decreases with increasing frequency within the range of 100–200 times/min. The CV of uniformity is less than 15% and the FDA is less than 5% at different speeds, thus meeting the requirements of fertilization uniformity and accuracy.

Table 7. Bench test results at different frequencies.

Operating Frequency of SRC X_3 /(times/min)	Y_1 /%	Y_2 /%
100	14.17	4.76
120	12.36	4.33
140	12.24	4.26
160	11.68	3.98
180	11.39	3.68
200	10.84	4.12

3.3.3. Fertilizer Crushing Rate Test Results at Different Frequencies

To investigate the fragmentation rate of granular fertilizers at different frequencies in bench tests, the fragmented fertilizers from each fertilizer-discharge performance test at different frequencies were collected and statistically analyzed. The fertilizer crushing rate (FCR) was calculated: the weight of the fragmented fertilizers was divided by the weight of the experimental fertilizers. The statistical results are shown in Figure 16. The results showed that the FCR increased with the increase in the operating frequency, but at different frequencies, the FCR in the bench test was less than 1%. Currently, there is no specialized industry standard or specification for the FCR of fertilizer-discharge machines. Based on the current quality-evaluation standard of fertilizer-discharge machines, as the FCR is less than 1%, it meets the requirements. The main reason for fertilizer breakage is that, during the SRC operation, it is easy for the fertilizer particles to be compressed between the gaps on the side walls of the fertilizer box, causing fertilizer particle breakage. Due to the particularity of strip fertilization, the FCR can affect the uniformity of fertilization and crop absorption efficiency. Therefore, it is recommended to reduce the FCR as much as possible and to control the operating frequency within the range of 100–200 times/min to protect granular fertilizer.

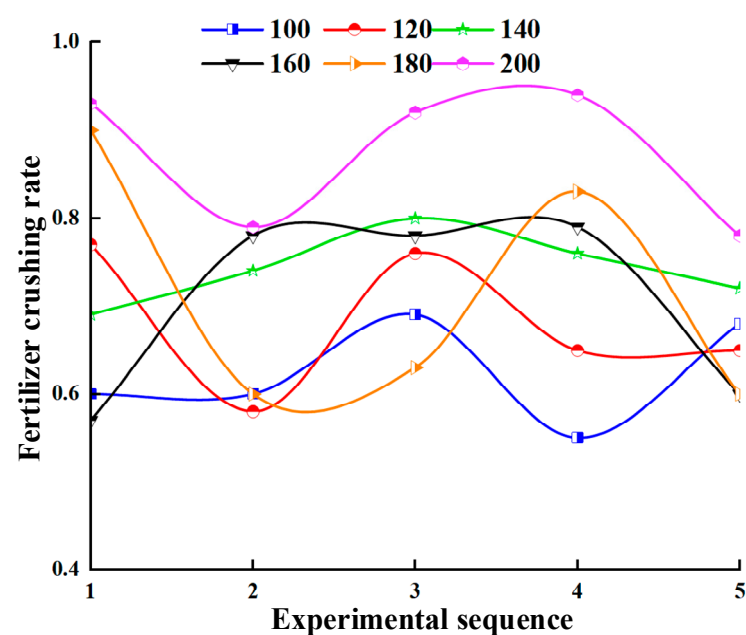


Figure 16. The statistical results.

3.4. Adaptability Test Results

Different fertilizers have different characterization parameters and flow characteristics. Fertilizers commonly used by farmers were selected to test the adaptability of the fertilizer discharge device to different types of fertilizers. The relevant parameters are shown in Table 8, and other experimental parameters are consistent with the above. Table 9 shows the results of the effects of different fertilizer varieties on fertilizer discharge performance. The results indicate that the fertilizer discharge device has good adaptability to different types of fertilizers.

Table 8. Basic physical parameters of three varieties of fertilizer granules.

Fertilizer Types	Equivalent Diameter/mm	Density (kg·m ⁻³)	Sphericity/%	Angle of Repose/°
Lanjingling	3.08	820.14	94	27.7
Changqingshu	3.19	1122.5	92	29.3
Shidanli	3.44	915.3	83	33.9

Table 9. Analysis of the adaptability of the fertilizer discharge device to three varieties of granular fertilizers.

Projects		Y ₁ /%	Y ₂ /%
Lanjingling	1	9.93	3.71
	2	9.74	3.69
	3	9.94	3.64
	Average value	9.87	3.68
Changqingshu	1	10.51	3.75
	2	10.25	3.69
	3	10.77	3.27
	Average value	10.51	3.57
Shidanli	1	10.87	3.52
	2	10.77	3.51
	3	11.15	3.65
	Average value	10.93	3.56

4. Discussion

In this study, a disturbance-type precision fertilizer-discharge device with a vertical pendulum for strip fertilization was designed to address the difficulties of smooth operation, stability, and poor uniformity of fertilizer discharge. Simulation experiments were conducted using the DEM, including response-surface orthogonal experiments to simulate the working state of strip fertilization and optimize the design parameters of the DFSD. The optimal parameter values of x_1 , x_2 , x_3 , and x_4 were determined: the wedge angle x_1 of the PMPB was 45°, the tilt angle x_2 of the APP was 46°, the FGPB x_3 of the SRC was 4.5 mm, and the combined operation frequency x_4 of the SRC was 188 times/min. At this point, the model predicted that the CV of fertilizer uniformity would be 10.53%, and that the FDA would be 3.19%. Finally, bench tests were conducted using the optimal parameters to verify the working effect of the optimized fertilizer-discharge device. The CV of fertilizer uniformity in the bench test was 11.06%, with a fertilizer accuracy of 3.51%. The relative error between the CV of fertilizer uniformity in the simulation test and the bench test was 0.53%, and the relative error between the FDA was 0.32%.

In order to improve the smoothness, stability, and uniformity of fertilizer application during the fertilization process of a strip fertilization device, Wang et al. [29] designed a vertical spiral-quantitative fertilizer-application machine, and the speed of the screw fertilizer application machine can automatically adapt to the moving speed. It can achieve precise control of fertilizer application, with an FDA of less than 4% and a CV of uniformity of less than 3%. This indicates that matching the speed of the fertilizer applicator to the

speed of the fertilizer applicator in quantitative fertilization operations can effectively improve the uniformity of fertilizer discharge. The device in this article is equipped with an eccentric pin shaft on the walking wheel of the fertilizer applicator to form a crank rocker transmission mechanism, which drives the SRC to perform a reciprocating motion, forcing the fertilizer to flow out from the fertilizer-discharge port. The reciprocating motion of the SRC is compatible with the speed of the fertilizer applicator, effectively improving the uniformity of fertilizer discharge. Wei et al. [30] designed a mechanical forced-fertilizer-discharge device. The machine uses an electric external groove wheel fertilizer-discharge device to discharge fertilizer into the fertilizer-discharge pipe. At the end of the fertilizer discharge, the fertilizer is forcibly discharged using a vertical spiral structure, solving the problem of easy blockage of the fertilizer discharge port during the operation of the fertilizer applicator. However, continuous rotation of the screw fertilizer applicator during operation may cause periodic changes in the gap between the screw and the casing around the fertilizer outlet, resulting in uneven fertilization. Therefore, a fixed-size fertilizer discharge port has a positive effect on the uniformity of fertilizer discharge, which is consistent with the design concept of the device in this study. Dun et al. [31] developed a circular arc gear fertilizer discharger and established a simulation model of its operation process. A comparative study was conducted on factors such as the speed and length of the fertilizer discharger, which affect the stability of fertilizer discharge. It was found that the minimum slot length (i.e., the fertilizer flow gap) between two circular-arc fertilizer dischargers has the most significant impact on the stability CV of fertilizer discharge, and its uniformity was greatly improved, which is consistent with the conclusion made in this paper that the FGFB is an important influencing factor on fertilizer-discharge performance. Liu et al. [32] designed a spiral cone centrifugal fertilizer discharger, which adopts a spiral disturbance cup structure, aiming to accelerate the flow speed of fertilizer and prevent blockage caused by the formation of fertilizer bridge arches. An experiment showed that its fertilizer stability coefficient was greater than 96%, and the CV was less than 5.57%. The use of disturbance structures to increase fertilizer flow velocity can effectively avoid fertilizer arching and blockage, providing ideas for the design of the disturbance SRC in the device in this study. Based on existing research ideas, a DFSD with a vertical pendulum bar was designed, and, through an EDEM simulation and bench tests, the feasibility and reliability of this device were demonstrated, providing new ideas for the development of precision-fertilization devices.

5. Conclusions

A disturbance-type precision fertilizer-discharge device with a vertical pendulum for strip fertilization was proposed in this study. The use of disturbance structures to increase fertilizer flow velocity can effectively avoid fertilizer arching and blockage, providing ideas for the design of the disturbance SRC in the device in this study. The fertilizer discharge device of DFSD is optimized using a combination of mathematical modeling, discrete element simulation, and experimentation. The results showed that the factors affecting the CV of uniformity and the FDA were the operating frequency of the SRC, the FGFB, the wedge angle of the PMPB, and the inclination angle of the toggle APP. After rounding, the wedge angle of the PMPB was 45° , the inclination angle of the APP was 46° , the operation frequency of the SRC was 188 times/min, and the FGFB was 4.50 mm. At this time, the model predicted that the CV of fertilizer uniformity would be 10.53%, and that the FDA would be 3.19%. A prototype of the fertilizer discharge device was developed and validated through bench tests. The results show that the CV of fertilizer uniformity was 11.06%, and that the FDA was 3.51%. The test results are similar to the predicted values of the model, verifying the accuracy of the simulation and the rationality of the prototype design. The fertilizer discharge device has good adaptability to different types of fertilizers. The research results can provide a reference for the development of precision strip fertilization devices.

Author Contributions: Conceptualization, L.C. and Z.L.; methodology, L.C. and Z.L.; software, Z.L.; validation, Z.L., L.C. and X.D.; formal analysis, L.C. and X.D.; investigation, X.M. (Xiangwei Mou) and R.C.; resources, X.M. (Xiangwei Mou); data curation, R.C.; writing—original draft preparation, Z.L. and X.D.; writing—review and editing, X.D.; visualization, Z.L.; supervision, Z.L.; project administration, L.C. and Z.L.; funding acquisition, X.M. (Xu Ma). All authors have read and agreed to the published version of the manuscript.

Funding: This work was supported by the Key Areas Research and Development Programs of Guangdong, grant number 2023B0202130001.

Institutional Review Board Statement: Not applicable.

Data Availability Statement: Data will be made available upon request.

Conflicts of Interest: The authors declare no conflicts of interest.

References

- Zhang, Y.; Xia, C.Z.; Zhang, X.Y.; Sha, Y.; Feng, G.Z.; Gao, Q. Quantifying the relationships of soil properties and crop growth with yield in a NPK fertilizer application maize field. *Comput. Electron. Agric.* **2022**, *198*, 107011. [[CrossRef](#)]
- Sun, X.B.; Niu, L.H.; Cai, M.C.; Liu, Z.; Wang, Z.H.; Wang, J.W. Particle motion analysis and performance investigation of a fertilizer discharge device with helical staggered groove wheel. *Comput. Electron. Agric.* **2023**, *213*, 108241. [[CrossRef](#)]
- Xi, X.B.; Wang, R.Y.; Wang, X.T.; Shi, Y.J.; Zhao, Y.; Zhang, B.F.; Qu, J.W.; Gan, H.; Zhang, R.H. Parametric optimization and experimental verification of multi-fertilizer mixing by air blowing and blade stirring based on discrete element simulations. *Comput. Electron. Agric.* **2023**, *210*, 107895. [[CrossRef](#)]
- Chen, G.B.; Wang, Q.J.; Xu, D.J.; Li, H.W.; He, J.; Lu, C.Y. Design and experimental research on the counter roll differential speed solid organic fertilizer crusher based on DEM. *Comput. Electron. Agric.* **2023**, *207*, 107748. [[CrossRef](#)]
- Villette, S.; Piron, E.; Miclet, D. Hybrid centrifugal spreading model to study the fertiliser spatial distribution and its assessment using the transverse coefficient of variation. *Comput. Electron. Agric.* **2017**, *137*, 115–129. [[CrossRef](#)]
- Heiß, A.; Paraforos, D.S.; Sharipov, G.M.; Griepentrog, H.W. Real-time control for multi-parametric data fusion and dynamic offset optimization in sensor-based variable rate nitrogen application. *Comput. Electron. Agric.* **2022**, *196*, 106893. [[CrossRef](#)]
- Patterson, D.E.; Reece, A.R. The theory of the centrifugal distributor. I: Motion on the disc, near-centre feed. *J. Agric. Eng. Res.* **1962**, *7*, 232–240.
- Cool, S.C.; Pieters, J.; Mertens, K.C.; Hijazi, B.; Vangeyte, J. A simulation of the influence of spinning on the ballistic flight of spherical fertiliser grains. *Comput. Electron. Agric.* **2014**, *105*, 121–131. [[CrossRef](#)]
- Lv, J.Q.; Sun, Y.K.; Li, J.C.; Li, Z.H.; Li, Z.Y. Design and test of vertical spiral organic fertilizer spreading device. *Trans. Chin. Soc. Agric. Eng.* **2020**, *36*, 19–28. [[CrossRef](#)]
- Shen, C.J.; Zhang, L.X.; Zhou, Y.; Dai, Y.M.; Li, F.; Zhang, J. Kinematic analysis and tests of the insertion mechanism of a self-propelled orchard gas explosion subsoiling and fertilizing machine. *Trans. Chin. Soc. Agric. Eng.* **2022**, *38*, 44–52. [[CrossRef](#)]
- Du, X.; Liu, C.L.; Jiang, M.; Yuan, H.; Dai, L.; Li, F.L. Design and Experiment of Inclined Trapezoidal Hole Fertilizer Point-applied Discharging Device. *Trans. Chin. Soc. Agric. Mach.* **2021**, *52*, 43–53. [[CrossRef](#)]
- Wang, J.F.; Fu, Z.D.; Weng, W.X.; Wang, Z.T.; Wang, J.W.; Yang, D.Z. Design and Experiment of Conical-disc Push Plate Double-row Fertilizer Apparatus for Side-deep Fertilization in Paddy Field. *Trans. Chin. Soc. Agric. Eng.* **2023**, *54*, 53–62. [[CrossRef](#)]
- Ulloa, C.C.; Krus, A.; Barrientos, A.; del Cerro, J.; Valero, C. Robotic Fertilization in Strip Cropping using a CNN Vegetables Detection-Characterization Method. *Comput. Electron. Agric.* **2022**, *193*, 106684. [[CrossRef](#)]
- Wang, J.F.; Wang, Z.T.; Weng, W.X.; Liu, Y.F.; Fu, Z.D.; Wang, J.W. Development status and trends in side-deep fertilization of rice. *Renew. Agric. Food Syst.* **2022**, *37*, 550–575. [[CrossRef](#)]
- Zhu, Q.Z.; Zhu, Z.H.; Zhang, H.Y.; Gao, Y.Y.; Chen, L.P. Design of an Electronically Controlled Fertilization System for an Air-Assisted Side-Deep Fertilization Machine. *Agriculture* **2023**, *13*, 2210. [[CrossRef](#)]
- Tang, H.; Jiang, Y.M.; Wang, J.W.; Wang, J.F.; Zhou, W.Q. Numerical analysis and performance optimization of a spiral fertilizer distributor in side deep fertilization of a paddy field. *Proc. Inst. Mech. Eng. Part C J. Mech. Eng. Sci.* **2021**, *235*, 3495–3505. [[CrossRef](#)]
- Bulgakov, V.; Pascuzzi, S.; Ivanovs, S.; Nadykto, V.; Nowak, J. Kinematic discrepancy between driving wheels evaluated for a modular traction device. *Biosyst. Eng.* **2020**, *196*, 88–96. [[CrossRef](#)]
- Adamchuk, V.; Lund, E.D.; Sethuramasamyraja, B.; Morgan, M.T.; Dobermann, A.; Marx, D.B. Direct measurement of soil chemical properties on-the-go using ion-selective electrodes. *Comput. Electron. Agric.* **2005**, *48*, 272–294. [[CrossRef](#)]
- Chen, Z. *Agricultural Machinery Design Handbook*; China Agricultural Science and Technology Press: Beijing, China, 2007; pp. 74–96.
- Zhu, H.B.; Wu, X.; Bai, L.Z.; Qian, C.; Zhao, H.R.; Li, H. Development of the biaxial stubble breaking no-tillage device for rice stubble field based on EDEM-ADAMS simulation. *Trans. Chin. Soc. Agric. Eng.* **2022**, *38*, 10–22. [[CrossRef](#)]
- Wang, Y.Y.; Chen, G.P.; Sun, H.; Liu, S.; Wang, C.; Hao, J.J. Design and experiments of a vertical aerobic composting reactor based on EDEM. *Trans. Chin. Soc. Agric. Eng.* **2023**, *39*, 171–179. [[CrossRef](#)]

22. Kang, Q.X.; Zhang, G.Z.; Zheng, K.; Liu, H.P.; Tang, N.R.; Liu, W.R.; Ji, C. Design and experiment of the spoon clip type seed metering device for *Allium chinense*. *Trans. Chin. Soc. Agric. Eng.* **2023**, *39*, 15–25. [[CrossRef](#)]
23. Liu, C.L.; Li, Y.N.; Song, J.N.; Ma, T.; Wang, M.M.; Wang, X.J.; Zhang, C. Performance analysis and experiment on fertilizer spreader with centrifugal swing disk based on EDEM. *Trans. Chin. Soc. Agric. Eng.* **2017**, *33*, 32–39. [[CrossRef](#)]
24. Sugirbay, A.M.; Zhao, J.; Nukeshev, S.O.; Chen, J. Determination of pin-roller parameters and evaluation of the uniformity of granular fertilizer application metering devices in precision farming. *Comput. Electron. Agric.* **2020**, *179*, 105835. [[CrossRef](#)]
25. Yang, Z.; Ou, Z.W.; Sun, J.F.; Duan, J.L.; Song, S.S.; Duan, J.; Song, S. Development of variable rate fertilizer applicator based on distribution characteristics of banana roots. *Trans. Chin. Soc. Agric. Eng.* **2020**, *36*, 1–10. [[CrossRef](#)]
26. Hu, J.; He, J.C.; Wang, Y.; Wu, Y.P.; Chen, C.; Ren, Z.Y.; Li, X.X.; Shi, S.J.; Du, Y.P.; He, P.X. Design and study on lightweight organic fertilizer distributor. *Comput. Electron. Agric.* **2020**, *169*, 105149. [[CrossRef](#)]
27. Song, C.C.; Wang, G.B.; Zhao, J.; Wang, J.H.; Yan, Y.; Wang, M.; Zhou, Z.Y.; Lan, Y.B. Research progress on the particle deposition and distribution characteristics of granular fertilizer application. *Trans. Chin. Soc. Agric. Eng.* **2022**, *38*, 59–70. [[CrossRef](#)]
28. Song, C.C.; Zhou, Z.Y.; Wang, G.B.; Wang, X.W.; Zang, Y. Optimization of the groove wheel structural parameters of UAV-based fertilizer apparatus. *Trans. Chin. Soc. Agric. Eng.* **2021**, *37*, 1–10. [[CrossRef](#)]
29. Wang, Y.; Xia, Z.L.; He, J.C.; Zhao, J.; Liu, H.B.; He, P.X. Design and Experiment of Quantitative Fertilizer Distributor with Vertical Screw. *J. Agric. Mech. Res.* **2018**, *40*, 88–92. [[CrossRef](#)]
30. Wei, G.J.; Qi, B.; Jiao, W.; Shi, S.; Jian, S.C. Design and Experiment of Mechanical Forced Fertilizing Device for Paddy Field. *Trans. Chin. Soc. Agric. Eng.* **2020**, *51*, 154–164. [[CrossRef](#)]
31. Dun, G.Q.; Ye, J.; Xia, W.Z.; Yang, Y.Z.; Yu, C.L.; Guo, Y.L.; Ji, W.Y. Design and simulation test of arc gear fertilizer apparatus. *J. China Agric. Univ.* **2019**, *24*, 111–120. [[CrossRef](#)]
32. Liu, X.D.; Lü, Q.Q.; Yang, L.Q.; Li, G.X. Design and Test of Peanut Root-Disk Full-Feeding Longitudinal Axial Flow Pod-Picking Device. *Agriculture* **2023**, *13*, 1103. [[CrossRef](#)]

Disclaimer/Publisher’s Note: The statements, opinions and data contained in all publications are solely those of the individual author(s) and contributor(s) and not of MDPI and/or the editor(s). MDPI and/or the editor(s) disclaim responsibility for any injury to people or property resulting from any ideas, methods, instructions or products referred to in the content.